Acupuncture mobilizes the brain's default mode and its anti-correlated network in healthy subjects

Published in final edited form as:
Brain Res. 2009 September 1; 1287: 84–103. doi:10.1016/j.brainres.2009.06.061.

Acupuncture mobilizes the brain's default mode and its anti-correlated network in healthy subjects

Kathleen K.S. Hui[1,*], **Ovidiu Marina**[1,2], **Joshua D. Claunch**[1], **Erika E. Nixon**[1], **Jiliang Fang**[1,3], **Jing Liu**[1], **Ming Li**[1], **Vitaly Napadow**[1], **Mark Vangel**[1], **Nikos Makris**[4], **Suk-tak Chan**[1,5], **Kenneth K. Kwong**[1], and **Bruce R. Rosen**[1]

[1]Athinoula A. Martinos Center for Biomedical Imaging, Department of Radiology, Massachusetts General Hospital & Harvard Medical School, Charlestown, Massachusetts

[2]School of Medicine, Case Western Reserve University, Cleveland, Ohio

[3]Guang An Men Hospital, Department of Radiology, China Academy of Traditional Chinese Medicine, Beijing, China

[4]Center for Morphometric Analysis, Department of Neurology, Massachusetts General Hospital & Harvard Medical School, Charlestown, Massachusetts

[5]Department of Health Technology and Informatics,The Hong Kong Polytechnic University, Hong Kong

Abstract

Previous work has shown that acupuncture stimulation evokes deactivation of a limbic-paralimbic-neocortical network (LPNN) as well as activation of somatosensory brain regions. This study explores the activity and functional connectivity of these regions during acupuncture vs. tactile stimulation and vs. acupuncture associated with inadvertent sharp pain. Acupuncture during 201 scans and tactile stimulation during 74 scans for comparison at acupoints LI4, ST36 and LV3 was monitored with fMRI and psychophysical response in 48 healthy subjects. Clusters of deactivated regions in the medial prefrontal, medial parietal and medial temporal lobes as well as activated regions in the sensorimotor and a few paralimbic structures can be identified during acupuncture by general linear model analysis and seed-based cross correlation analysis. Importantly, these clusters showed virtual identity with the default mode network and the anti-correlated task-positive network in response to stimulation. In addition, the amygdala and hypothalamus, structures not routinely reported in the default mode literature, were frequently involved in acupuncture. When acupuncture induced sharp pain, the deactivation was attenuated or became activated instead. Tactile stimulation induced greater activation of the somatosensory regions but less extensive deactivation of the LPNN. These results indicate that the deactivation of the LPNN during acupuncture cannot be completely explained by the demand of attention that is commonly proposed in the default mode literature. Our results suggest that acupuncture mobilizes the anti-correlated functional networks of the brain to mediate its actions, and that the effect is dependent on the psychophysical response.

[*]Corresponding author: Kathleen K.S. Hui, Athinoula A. Martinos Center for Biomedical Imaging, Department of Radiology, Massachusetts General Hospital, 149 13th St., Charlestown, MA 02129 Tel: (617) 724-7194 .Fax (617) 726-7422 hui@nmr.mgh.harvard.edu.

Keywords

acupuncture; fMRI; limbic-paralimbic-neocortical network; default mode network; *deqi*; amygdala

1. Introduction

Recent PET and fMRI studies indicate that the brain is organized into two anti-correlated functional systems on the global level (Fox et al., 2005; Fransson, 2005). The term anti-correlated is used because as one of the networks increases in activity (activation or task-positive network), the other shows coherent decrease in activity (deactivation or task-negative network). The task-negative network, commonly called the default mode network (DMN), is comprised of cortical and subcortical structures in the medial prefrontal cortex (MPFC), medial parietal cortex (MPC) and medial temporal lobe (MTL) that are highly active in the resting state (awake and conscious) but become deactivated when exposed to external stimuli such as cognition and conceptual tasks (Binder et al., 1999; Buckner et al., 2008; Fransson, 2005; Golland et al., 2008; Gusnard and Raichle, 2001; Shulman et al., 1997). The task-positive network is comprised of the sensorimotor and attention-related cortices that become activated during goal-directed tasks (Corbetta and Shulman, 2002).

It is suggested that the DMN involves a mode of preparedness and alertness for possible changes in the internal milieu or external environment, and the integrity of the DMN and its anti-correlated network may be central to the balance of brain functions and maintenance of health. Its role in health and disease has recently become a subject of intense research interest.Its clinical relevance is indicated by the growing number of reports on its involvement in cognitive, affect and behavioral disorders, such as Alzheimer's disease (Greicius and Menon, 2004; He et al., 2007; Lustig et al., 2003; Rombouts et al., 2005; Wang et al., 2006), autism (Kennedy and Courchesne, 2008; Kennedy et al, 2006), schizophrenia (Bluhm et al., 2007; Liang et al., 2006; Zhou et al., 2007), major depression (Anand et al., 2007), attention deficit hyperactivity disorder (Cao et al., 2006; Castellanos et al., 2008; Zang et al., 2007); multiple sclerosis (Lowe et al., 2002) and Parkinson's disease (Stoffers et al., 2007). These studies have shown alterations in the generalized activity and functional connectivity of the DMN in patients with these disorders

While the exact neurocorrelates of acupuncture's clinical effects remain unclear, clinical and experimental data suggest that the effects of acupuncture are mediated via internal regulatory networks of the central and peripheral nervous systems (Cheng, 2000; Han, 2003). Functional MRI studies from our group and others (Hui et al., 1997, 2000, 2005; Fang SH et al., 2006, Fang JL et al., 2008, Napadow et al., 2005, Wang et al., 2007, Wu et al., 1999) have revealed that acupuncture induces extensive deactivation of limbic regions and moderate activation of somatosensory regions, which show virtual identity with the deactivation and activation networks of the resting brain in response to attention-demanding tasks. The increasing recognition of the crucial role of inhibition in the regulation of neuronal activity to maintain a state of balance points to the important role of the task-negative LPNN in acupuncture action. We hypothesize that acupuncture may mediate its diverse regulatory effects by promoting deactivation of the DMN and that additional limbic regions important to emotional processing and regulation may participate more often in acupuncture than in cognition and conventional sensory stimulation. Moreover, according to traditional Chinese Medicine, acupuncture's clinical efficacy is related to the unique psychophysical response, termed *deqi*, which is comprised of feelings of aching, soreness, et cetera. We further hypothesize that acupuncture's effects on the LPNN would be influenced by the psychophysical response.

To test these hypotheses, the data of manual acupuncture with fMRI monitoring and tactile stimulation for sensory comparison at LI4 (*hegu*) on the hand, ST36 (*zusanli*) on the leg, and LV3 (*taichong*) on the foot were retrieved for analysis with a total of 201 acupuncture scans on 48 subjects. These are the most commonly used acupoints in clinical practice and are often employed separately or in combination for their analgesic and regulatory clinical effects (Napadow et al., 2004). After observing marked similarity in the blood oxygen level dependant (BOLD) response across these acupoints, the data was combined for further analysis in order to obtain a general pattern of response to treatment at three frequently used acupoints. While many mathematical systems models have been used to show the various functional networks of the brain, we applied the most commonly used model, seed-based cross correlation analysis (CCA), to demonstrate the functionally connected voxels at different levels of the brain during acupuncture needle manipulation. Because of the criticism that the results of seed-based analyses may be influenced by the paradigm, the results from CCA were cross checked with the model free probabilistic independent component analysis (pICC). The networks with coherent activation and deactivation were compared to those described for the resting brain in the literature. We also propose that the deactivation of the LPNN during acupuncture could involve a mechanism besides the demand of attention alone.

2. Results

Data were collected from 51 healthy right-handed, acupuncture-naïve subjects. The fMRI data from 3 subjects were discarded due to excess motion artifacts, resulting in 48 subjects (20-47 year old, mean=28.6±7.56SD, 19 M, 29F) who provided hemodynamic as well as psychophysical data during acupuncture and tactile stimulation at three acupuncture points for analysis.

2.1. Psychophysical Response

The *deqi* response (aching, soreness, pressure, heaviness, fullness, warmth, coolness, numbness, tingling, or dull pain) was significantly more common in acupuncture (71% of scans) than in superficial tactile stimulation (24%), and most tactile *deqi* consisted of surface tingling. *Deqi* was mixed with brief episodes of sharp pain in 15% of acupuncture and in 2% of tactile stimulation**.** Five percent of acupuncture and 74% of tactile stimulation elicited no *deqi* sensations. The psychophysical response of 42 of the subjects was presented in detail in a recent report (Hui et al., 2007).

2.2. Hemodynamic response

Forty-eight subjects who received acupuncture in a total of 201 scans (37 subjects in 64 scans at LI4, 43 subjects in 73 scans at ST36, 37 subjects in 64 scans at LV3) were analyzed. The general linear model (GLM) uses the periods where the acupuncture needle is in place as a baseline to assess the BOLD signal change during needle manipulation (bilateral manual rotation of the needle of 180 degrees at 1 Hz). The mean % change in the signal intensity of the peak voxels and the variations (t values) between the datasets are presented for the structures of each group. The general pattern of hemodynamic response observed using GLM was remarkably similar in temporal and spatial characteristics across the points although the intensity, extent and preferential localizations showed variations, with LI4 eliciting the strongest response (Fig 1). Clusters of deactivated regions appeared in the MPFC, MPC, and MTL for all the acupoints. The MPFC regions can be divided into the frontal pole and pregenual cingulate at the midlevel and the subgenual cingulate, ventromedial prefrontal cortex, orbito-frontal cortex and subgenual area SG25 at the ventral level. The precuneus, posterior cingulate BA31, BA23 ventral (BA23v) and retrosplenial cortex BA29/30 formed confluent areas of deactivation in the MPC. Deactivation of the

amygdala, hippocampus and parahippocamus in the MTL were best seen in the coronal sections. Signal decreases also occurred in the angular gyrus, cuneus, hypothalamus, pontine nuclei, cerebellar vermis and tonsil. Compared to the widespread deactivation network, the task-positive network was more limited in distribution and comprised of regions of heterogeneous functions. The thalamus, sensorimotor, unimodal association and attention-related cortices including the secondary somatosensory cortex (SII), dorsolateral prefrontal cortex_BA9, BA6, BA22, and BA37 demonstrated activation for all three acupoints.

In an attempt to understand acupuncture's effects across three commonly used TCM acupoints, data for all three acupoints were combined for group analysis. Subtle differences between acupoints are being analyzed for a future study. The combination of the data for all 3 points for analysis in this study has brought new information on the generalized effects of acupuncture across commonly used acupoints both in the task-negative and task-positive networks allowing for comparison with tactile stimulation and acupuncture involving inadvertent sharp pain. The ST36 data collected from 15 of the participants were presented in an earlier report (Hui et al., 2005).

2.3 Acupuncture vs. tactile stimulation

Comparison of the task-negative and task-positive networks of acupuncture and tactile stimulation performed on matched acupoints in 37 subjects revealed similarities as well as differences (Table 1, Fig 2). For the task-negative network, the aggregates of deactivated structures in the MPFC and MPC showed substantial overlap between the two procedures, but the response was more prominent in acupuncture as measured by the average change in signal intensity (paired t values and % of signal change in the peak voxel) and by the extent of involvement (the percentage of the total volume affected in the structure). In acupuncture, the decrease in signal intensity was most marked in the VMPFC (SG25, orbito-frontal cortex, subgenual cingulate), followed by the precuneus, posterior cingulate, temporal pole and hypothalamus, and weakest in the structures of the MTL. The extent of involvement was as high as 90% of total voxels in the precuneus, posterior cingulate, followed by the pregenual cingulate, SG25 (50%), frontal pole, orbito-frontal cortex, subgenual cingulate, and hypothalamus (50-31%), dorsolateral prefrontal cortex, BA39, hippocampus, parahippocampus (30-10%) and amygdala (8%). In tactile stimulation, the change in signal intensity and the extent of involvement of the different structures appeared in the same order as in acupuncture, but the overall response was much weaker. The most significant difference between the acupuncture and tactile stimulation was seen in the frontal pole, pregenual cingulate, and hypothalamus ($p < 0.01$).

In the task-positive network, activation of the somatosensory (contralateral SII) and association cortices was more marked in tactile stimulation than in acupuncture ($p < 0.01$) while activation of subcortical and paralimbic structures (thalamus, right anterior insula, anterior middle cingulate and posterior cingulate BA23d) was observed only in acupuncture, not in tactile stimulation when thresholded at $p < 0.0001$.

2.4 Noxious stimulation

The group data of acupuncture with *deqi* derived from 52 scans in 37 subjects at the three acupoints was compared with the same number of scans that evoked concomitant sharp pain in 29 subjects with a voxel by voxel two sample t-test. The prominent deactivation induced by *deqi* in most core regions of the DMN, such as the posterior cingulate BA31, precuneus, orbito-frontal cortex, temporal pole, right amygdala, hippocampus, and parahippocampus were significantly attenuated in the presence of sharp pain ($p < 0.05$). The hypothalamus, left amygdala and cerebellar vermis even became activated (Fig 3, Table 2A). The pregenual cingulate and SG25 showed less deactivation (Fig 3) and less consistency in the magnitude

of signal decrease as measured by the t values of the peak voxels (Table 2A). The dorsomedial prefrontal cortex showed activation during sharp pain but not during *deqi* (Fig 3). In the task-positive network, activation of the paralimbic antero-middle cingulate BA32/24 and posterior cingulate BA23 dorsal (BA23d) as well as the somatosensory cortices BA40, 43 were all augmented in the presence of sharp pain. Activation of the insula in sharp pain could occur in any division of the insula on any side of the brain, while its activation in *deqi* was localized to the right anterior division (Fig 3, Table 2B).

2.5 Functional connectivity

While various mathematical models have been used to explore neurological connectivity, we found seed-based cross correlation analysis (CCA) to be the most appropriate for our data. Seed-based CCA uses the average time-course (BOLD activity over the 10 minute paradigm) of a reference region (a sphere with a radius of 4.5mm) to compare with every other voxel in the brain. While the general linear model imposes our stimulation paradigm onto the data, CCA has the benefit of using one region of the brain as the comparison tool. Theoretically, if two regions of the brain fluctuate together over an extended time period, they are believed to be “functionally connected”.

2.5.1. Seed-based cross correlation analysis—With the use of seeds from the task-negative network, coherent low frequency BOLD fluctuations were observed in the posterior cingulate, precuneus, retrosplenial cortex, frontal pole, pregenual cingulate, subgenual cingulate, SG25, temporal pole, hippocampus, parahippocampus, angular gyrus, and cerebellar vermis in both hemispheres during needle manipulation (Fig. 4.1 a-f). The regional correlations showed virtual identity with the core regions of the DMN in the MPC, MPFC and MTL (Buckner et al., 2008; Fox et al., 2005; Fransson, 2005). In addition, the amygdala, hypothalamus, cerebellar vermis and brain stem nuclear groups that are not often mentioned in the DMN literature also demonstrated coherent activity with these DMN core regions. The strength of correlation and the extent of involvement in seed-based CCA varied with the use of different reference regions. In acupuncture, the use of BA31 and SG25 as references showed the strongest regional coherence and similarity in spatial characteristics (Fig 4.1.a, c), a finding with potentially significant implications (Greicius et al., 2003). The use of pregenual cingulate, hippocampus and hypothalamus as references demonstrated coherent activity in similar regions but with weaker correlation coefficients. The hypothalamus, however, showed strong coherence with the orbitofrontal cortex and subgenual areas (Fig 4.1.f), a finding that is compatible with the strong anatomical connections between these regions (Drevets, 2007). The amygdala demonstrated the weakest regional coherence among all the seeds tested, coherent activity was readily identifiable in the MPC and VMPFC nearby but sparse in more remote regions such as the posterior cingulate and the more dorsal regions of the MPFC (Fig 4.1.e).

In tactile stimulation, regional coherence was also observed for seeds from the deactivation network, with the exception of the amygdala. However, the brain volumes involved were more limited and the correlation coefficients were weaker than in acupuncture. Among the seeds tested, SG25 showed the greatest coherent activity.

Using the left SII (contralateral to the site of stimulation) as a reference region for the activation network, both acupuncture and tactile stimulation elicited coherent activation in the thalamus, right SII, and association cortices in lateral prefrontal and temporal lobes. Notably, activation of the SII and several association cortices was more prominent in tactile stimulation than in acupuncture (Fig 4.2a). This contrasts with the task-negative system, in which deactivation was much more pronounced in acupuncture. Using SII as a seed, significant coherent activity of the right anterior insula, antero-middle cingulate and

posterior cingulate BA23d, was seen in acupuncture, but not seen (right anterior insula, antero-middle cingulate) or much reduced (posterior cingulate BA23d) in tactile stimulation (Fig 4.2a). The sensory components of the task positive network responded more strongly to tactile stimulation while the paralimbic components responded more strongly to acupuncture.

2.5.2. Probabilistic independent component analysis (pICA)—Unlike a general linear model (which uses our predetermined time-course) or seed-based cross correlational analysis (which uses the time-course of a predetermined seed region), probabilistic independent component analysis is a program that automatically finds coherent patterns in BOLD fluctuations throughout large portions of the brain that reach statistical significance. The use of model-free pICA to cross check our GLM and seed-based CCA revealed a striking similarity of results between the methods. The clusters of deactivated regions in the MPFC, MPC, and MTL by pICA (Fig 5A) were almost identical in temporal and spatial characteristics to those demonstrated by GLM (Figs 1-3&6) and CCA (Fig 4). The amygdala and hypothalamus were involved in all the methods. The distribution of activated regions in the SII, dorsolateral prefrontal cortex, and middle cingulate/posterior cingulate BA31 regions was also similar between pICA (Fig 5B) and CCA (Fig 4.2). The time-course by pICA showed near perfect agreement with the paradigm for the deactivation system (Fig. 5A). As for the activation system, the maximal response by pICA was delayed and differed in intensity between the two episodes of acupuncture stimulation (Fig 5B).

2.5.3. Global views—The similarity of the spatio-temporal behavior of the LPNN during acupuncture *deqi* and the DMN of the literature can be readily appreciated by comparing the statistical maps of acupuncture fMRI with a well-known map of the default system (Shulman et al., 1997). Synthesis of the sagittal views of the BOLD response deactivation network for the 48 acupuncture subjects demonstrates regions in the MPFC, MPC and temporal lobe that are representative of the DMN (Fig 6a). (The 3D views of the surface of the brain and of a coronal section through the anterior commissure obtained by SUMA (Surface Mapper. AFNI) demonstrate the task-negative network in the prefrontal, parieto-occipital and temporal lobe regions depicted in blue separated by the task-positive network in the fronto-parietal regions depicted in red (Fig 6b).

3. Discussion

3.1 Confirmation and extension of previous findings

Previous studies by our group and others have shown a generalized deactivation of the LPNN across multiple levels of the brain and activation of the sensorimotor system during acupuncture stimulation (Hui et al., 1997, 2000, 2005; Fang SH et al. 2006, Fang JL et al., 2008, Napadow et al. 2005, Wang et al. 2007, Wu et al., 1999). With the increased statistical power of this accumulative study, more thorough analysis and the application of functional connectivity analysis, we were able to confirm and extend our previous findings to provide a general hemodynamic response for multiple acupoints with common analgesic and regulatory actions. Using CCA, we have demonstrated the concomitant presence of a deactivation network and an activation network that are negatively correlated to each other in their temporal characteristics, and that both networks show substantial convergence with the deactivation and activation networks described in the resting brain literature. In addition, we observed interesting details about the major brain structures involved in acupuncture action and how they correlate with one another, leading us to new understandings about the systems and sub-systems involved. The results strongly suggest that acupuncture may mobilize these intrinsically organized dynamic functional systems to mediate its diverse effects.

3.2.1 Task-negative network—The clusters of deactivated regions in the MPFC (pregenual cingulate, subgenual cingulate, frontal pole, VMPFC, SG25), the MPC (precuneus, posterior cingulate BA31, 29, 30, 23v), the hippocampal formation and the angular gyrus during acupuncture showed marked resemblance to the spatio-temporal characteristics of core regions in the DMN as described in the literature. A difference was, however, noted in two important limbic structures, the amygdala and the hippocampus; their involvement was much more frequent in acupuncture than in cognitive tasks in the literature. The striking similarities between the findings by the different approaches in analysis, the GLM, CCA, and pICA, bolster our confidence on the validity of the results.

A comparison of these results with the BOLD patterns during tactile stimulation have revealed some interesting findings, and help to distinguish which regions are preferentially affected by the more superficial stimulation and which are unique to acupuncture. While coherent deactivation was also seen in tactile stimulation in a subset of the task-negative network, it was significantly weaker and more limited in extent and probably would not have reached statistical significance if the sample size had not been as large. The difference between acupuncture and tactile stimulation was especially marked in the posterior cingulate and precuneus of the MPC and in the pregenual cingulate bilaterally; it was less marked in the SG25 area. The results suggest the presence of subsystems that differ in their sensitivity to the two types of sensory stimuli, acupuncture and tactile stimulation, and that the pregenual and posterior parietal regions may represent the structures most unique to acupuncture action. It has been suggested that subsystems may exist within the anti-correlated networks of the resting brain (Golland et al., 2008). The pregenual cingulate is involved in disorders of emotional regulation such as depression (Anand et al 2007). The posterior cingulate and precuneus in the MPC are involved in cognitive disorders, as well as affect or behavioral disorders with a cognitive element. Failure of these regions to deactivate during cognitive tasks is one of the early symptoms of Alzheimer's disease (Rombouts et al., 2005). Future analysis of acupuncture on patients with these disorders will shed more light on acupuncture's mobilization of these networks in clinical settings.

The deactivation of the amygdala and hypothalamus in acupuncture but not in tactile stimulation suggests the important role of these major limbic structures in acupuncture action. To our knowledge, the hypothalamus was included in only one report (Greicius et al., 2003) while the amygdala was included in only two reports (Lowe et al., 1998; Shulman et al., 1997) among the many publications of cognitive tasks on the DMN. The regional coherence described for the structures was even more limited in distribution than what was seen in the present study with acupuncture. The hypothalamus and amygdala are central to the regulation and control of emotion and autonomic functions, and are generally activated by stress, pain and emotions of negative valence. In our acupuncture fMRI study on the carpal tunnel syndrome, these limbic structures showed more pronounced response in patients compared to healthy adults (Napadow et al., 2007). Most DMN studies in the literature have employed cognitive or perceptual tasks with little involvement of emotional or autonomic control. As mentioned above, the LPNN may contain subsystems that respond differently to different modalities of stimulation. The amygdala and hypothalamus may reflect a subsystem with preferential effects characteristic of acupuncture.

The coherent deactivation of the temporal pole with most reference regions in this study also appeared to be more extensive than reports in the DMN literature. The strong functional connectivity could be related to its close anatomical interconnections with other MTL and VMPFC regions. The temporal pole may play an important role in memory and social emotional processing (Kahn et al., 2008; Olson et al., 2007). In brief, the frequent involvement of the amygdala, hypothalamus and temporal pole in acupuncture may

comprise a subsystem either within the DMN or beyond the DMN that is mobilized by acupuncture.

3.2.2 Underlying mechanism—The mechanism underlying the extensive deactivation of the LPNN/DMN by acupuncture is unclear. It is believed that the DMN is preferentially active when individuals are not focused on the external environment and interruption of the activity by attention demanding tasks leads to inhibition of the activity of the system (Buckner et al., 2008). Our findings suggest that such an explanation cannot fully account for the phenomenon in acupuncture. Subjects would pay a certain amount of attention to the sensations elicited by the acupuncture or tactile stimulation, but the attention would be less demanding during innocuous sensations than during sharp pain. If attention or focus were the key factor in DMN deactivation, the attention caused by sharp pain would induce a stronger response. On the contrary, pain led to attenuation of the LPNN deactivation and even activation of several structures. Moreover, the anatomical distribution, though similar, showed differences for acupuncture and attention tasks. Limbic structures strongly related to affect and emotional regulation such as the hypothalamus and amygdala are frequently involved in acupuncture but only in isolated reports of cognitive tasks in the DMN literature. We posit that acupuncture may exert a direct effect on the limbic system to modulate its activity besides the demand of attention. It may inhibit the activity of a subsystem in the DMN that is more related to the affect, including the affective dimension of pain. We have also considered that the motion of raising fingers during sharp pain might affect the hemodynamic response, but subjects who experienced a strong level of *deqi* also raised their fingers. Moreover, any movement in both groups was only momentary and would not have a significant effect on our extended paradigm.

The widespread functional connectivity of the DMN and LPNN observed in acupuncture appears to have an anatomical basis supported by structural connectivity demonstrated by multiple approaches (Buckner et al., 2008; Honey et al., 2009). In addition to the gold-standard anterograde and retrograde tracer studies in animal models, including non-human primates (Schmahmann and Pandya, 2006), a recent study provided a large scale map of the interconnections between the core components of the DMN in the macaque (Parvizi et al., 2006). Furthermore, modern techniques in diffusion tensor and diffusion spectral imaging have enabled demonstration *in vivo* of the major white fiber paths of these circuits. Data on non-human primates demonstrate that the cingulum bundle and the uncinate fasciculus provide a loop with branching tracts that interconnect a multitude of nodes in the MPFC, MPC, retrosplenial cortex, and TL, while the stria terminalis and fornix directly connect the hypothalamus with the amygdala and hippocampus (Mori and van Zijl., 2007; Schmahmann et al., 2007). Most recently, these limbic nerve fiber bundles have been demonstrated in healthy human subjects with diffusion tensor and spectral tractography (Fujiwara et al., 2008; Greicius et al., 2008, Honey et al., 2009).

3.3.1 Activation network—The activation of the sensorimotor cortex, association cortices, the right anterior insula, supplementary motor area, antero-middle cingulate and the posterior cingulate BA23d during acupuncture showed overlap with the task-positive network described for the resting brain (Fox et al., 2005; Fransson, 2005). Activation of the sensorimotor cortex by acupuncture and augmentation in the presence of sharp pain is to be anticipated. However, our finding that acupuncture with invasive needling evoked less activation of the lateral sensorimotor and association cortices than gentle tapping with a flexible nylon monofilament is intriguing (Hui et al., 2000, 2005).

3.3.2 Mechanism—Contrary to conventional expectation, our fMRI studies have repeatedly indicated that the deactivation of the limbic system played the predominant role in acupuncture action and that such effects were not entirely dependent on sensorimotor

cortex activation. We hypothesize that impulses from acupuncture or from tactile stimulation can ascend by separate paths to activate the sensorimotor and association cortices or to modulate the limbic system and DMN. Activation of the sensorimotor cortex is primarily mediated by impulses ascending via the dorsal column medial leminiscal system while modulation of the limbic system is primarily mediated by impulses ascending in the spinocervical, spinoreticular and spinomesencephalic tracts (Willis & Westlund, 2004). Work in animal models including non-human primates have demonstrated that axons in these fiber tracts send collaterals to synapse directly with neurons in the dorsal thalamus, dorsal midbrain, medullary and pontine reticular formation, hypothalamus, amygdala, septum and nucleus accumbens of the limbic system (Willis 1989; Willis and Westlund 1997). Depending on the nature of the stimulus and the peripheral sensory receptors and nerve fibers at the site of stimulation, the proportion of impulses ascending by different paths and reaching different supraspinal targets will vary, which will lead to differences in the predominant effect on the brain. We postulate that a greater proportion of the impulses generated by acupuncture may reach the limbic system to exert its modularity effect while a greater proportion of the impulses generated by tactile stimulation may reach the sensorimotor cortex to exert its excitatory effect (see Fig 7a, tracts A and B). This could explain the overlap of both activation and deactivation effects as well as differences in the predominance of effects between these two procedures.

This is the first study to thoroughly analyze the divisions of the cingulate in relation to acupuncture's effects. In a previous study, we observed activation of the middle cingulate and posterior cingulate BA23d during electroacupuncture but not during manual acupuncture at ST36 in 15 subjects (Napadow et al., 2005). A similar effect is now demonstrable in manual acupuncture across multiple acupoints with increase in sample size. This finding overlaps with the task-positive network of the resting brain (Fox et al., 2005). The partition of these divisions of a paralimbic structure into a deactivation and an activation network that are anti-correlated to each other can be explained by their differences in cytoarchitecture and functions (Vogt, 2005; Vogt et al., 2003; Vogt et al., 2006). The middle cingulate involved in attention and pain perception and the BA23d involved in sensorimotor and evaluative functions are activated, while the rostral divisions involved in emotion and autonomic processing pregenual and subgenual cingulate, and the caudal divisions involved in self-reference assessment, posterior cingulate _BA31, 23v, are deactivated by acupuncture.

As mentioned above, unique activation of the right anterior insula is intriguing and is incompletely understood. Its activation by acupuncture appeared to depend on the acupoint and the stimulation technique. In manual acupuncture, the response was strong for LI4 and LV3 but did not reach significance for ST36. However, in a previous study from our group, the response was demonstrable for ST36 electroacupuncture at both low and high frequencies. The differences between acupoints may be attributed to differences in relative sensitivities rather than an all-or-none phenomenon.

3.4 Relationship between deactivation and activation networks

The presence of subsystems has been proposed for the anti-correlated networks of the resting brain (Golland et al., 2008). The comparisons of acupuncture *deqi* with conventional tactile stimulation and noxious stimulation suggest that there may be multiple variables and sub-systems involved. Among the regions of the task-positive network, a subset of regions including the right anterior insula, the thalamus, the antero-middle cingulate and the posterior cingulate BA23d – all limbic-related structures – appear to be more strongly connected and anti-correlated with the task-negative network than the subset comprised of sensorimotor and association cortices. Their anti-correlation may mean that one system acts to inhibit the other, and that the activation of these paralimbic regions sends inhibitory

signals to the LPNN, or that the LPNN normally inhibits the task-positive structures, and this inhibition is attenuated during acupuncture stimulation. These limbic related task-positive structures show strong responses to acupuncture *deqi*, with and without noxious pain, but markedly less response in tactile stimulation. Meanwhile, the sensorimotor and association cortices may form another sub-system that responds more to tactile stimulation and noxious pain than to acupuncture *deqi*.

It is suggested that the anti-correlation between the DMN and the task-positive networks may reflect the dichotomy between increased brain activity in regions supporting execution of a task and decreased brain activity in regions involved in unrelated processes, and that their relationship would influence behavioral performance (Fox et al., 2005). The interactions between these anti-correlated networks and the direction of influence are therefore important aspects of functional organization of the brain. Advances in fMRI analysis have provided modeling methods for exploring the effective connectivity or cause and effect relationships between anti-correlated networks as well as between nodes within an individual network. Recent results from Granger causality analysis suggest that the VMPFC and posterior cingulate of the DMN exert greater influence on their anti-correlated networks than the other way around (Uddin et al., 2008).

A recent preliminary report on the effect of acupuncture on the resting brain from our Center (Dhond et al., 2008) is supportive of the findings of the present study. Work is in progress to explore the effective connectivity within and between these anti-correlated systems.

3.5 Overview of the anticorrelated networks involved in acupuncture action

We will attempt to integrate our findings on the human brain during acupuncture with a schematic line drawing that illustrates the major cortical and subcortical regions of the deactivation and activation networks, accompanied by drawings of MRI sections that show the corresponding structures. Their components and their interconnections have been fully discussed above (See Sections 2.5, 3.3). A greater proportion of the impulses generated by acupuncture may ascend by the spinocervival, spinoreticular and spinomesencephalic tracts (Fig 7a, tract A) to reach the corticolimbic regions, while a greater proportion of the impulses generated by tactile stimulation and pain may ascend by the spinothalamic tract (Fig 7a, tract B) to reach the sensorimotor cortex (See Section 3.3.2). More detailed explanations are provided in the legend for the figure.

3.6 Clinical relevance

A growing number of mental disorders are reported to involve dysfunctions of the DMN, with disruptions of the functional connectivity and hyperactivity of major limbic regions, such as major depression (Anand et al., 2007; Mayberg, 2003; Mayberg, 2007), post-traumatic stress disorder (Stam, 2007), attention deficit hyperactivity disorder (Cao et al., 2006; Zang et al., 2007), autism (Kennedy et al. 2006), Alzhemimer's disease (Rombouts et al., 2005) as discussed in the Introduction. Our results suggest that acupuncture may mobilize the interactions between major limbic structures to enhance deactivation or suppress neuronal activation by stress, pain or other negative stimuli. Preliminary results of randomized controlled trials suggest that acupuncture may be effective in the treatment of major depression (Leo and Ligot, 2007) and post traumatic stress disorder (Hollifield et al., 2007). The results of our study should lead to a better understanding of the neurological correlate of acupuncture's effects in the clinical setting.

3.7 Experimental control

The design of a valid control for acupuncture is fraught with difficulties. Since the distribution of neural elements is ubiquitous, the use of a nearby non-point (not on any

meridian) for control cannot be viewed as inert or inactive (Dincer & Linde 2003, Complement Ther Med; Lund and Lundeberg, 2006; Kong et al, 2009). There is no consensus as to the proper selection of a non-point, for example, how far from the classical acupoint in use, the minimal distance from another meridian point in the neighborhood, and how different in histological components and segmental innervations. In our exploration for a non-point control in our early acupuncture fMRI studies, the response of the point chosen was very variable, ranging from minimal to pronounced response. Although successful use ofnon-points as control is purported by many authors, reports are emerging that fail to find significant differences between non-points and real acupoints (Fang et al, 2008). The common practice of placebo needles for sham acupuncture is also fraught with difficulties (Tsukayama et al., 2006, White et al., 2003). We, therefore, have opted to deliver superficial tactile stimulation to the acupoint, not as an inert control but as a means to help understand how acupuncture compares with a conventional form of sensory stimulation (Hui et al, 2000, 2005; Napadow et al. 2005, 2007). A recent study suggests tactile stimulation to be a “better control paradigm to extract the acupuncture specific brain responses”, which is in support of our findings (Ho et al., 2008).

3.8 Acupuncture techniques

Acupuncture action is very complex and is dependent on multiple factors that would need investigations by different methods using different controls to accomplish different objectives. The needling techniques of acupuncture may vary between acupuncturists. We have attempted to minimize this variability by having all the procedures performed by the same acupuncturist throughout the study. The results of this study apply to manual acupuncture stimulation with gentle needle rotation that aims to generate *deqi* without hurting the subject. The results may not apply to other needling techniques and particularly when subjects experiencing sharp pain are not separated from the major cohort in the data analysis. This will be particularly true of limbic regions associated with emotional processing and the affective dimensions of pain. Such differences in methodology may contribute to discrepancies in the hemodynamic response in acupuncture neuroimaging literature. Activation of the hypothalamus instead of deactivation has been reported by other groups in the literature (Wu et al, 1999, Liu et al., 2007). We opted to place the priority of our study on manual acupuncture because it has the longest history and is most commonly used in clinical settings, at least in China (Napadow et al., 2004). The effects of stimulation by other modalities such as electroacupuncture will require separate investigation. We have chosen acupoints that are most widely used for their analgesic and modulatory effects. Other acupoints with different histological and nerve supply characteristics remain to be explored.

3.9 Functional Connectivity

The use of functional connectivity models, such as CCA and pICA, to explore the neurological functioning of healthy patients in response to acupuncture stimulation is imperfect because it neither gives the direct path of connectivity (as in structural connectivity methods like diffusion tensor tractography) or the direction of influence (as in effective connectivity methods like structural equation modeling and Granger causality). A recent editorial article discussed the benefits and limitations of each of these mathematical systems models (Stephan et al., 2008). While seed-based CCA is more commonly used, it is limited in that the inspector must choose a seed as a reference region, which may reflect inspector bias. It is for this very reason that we cross-checked the results obtained by seed-based CCA with pICA, a model-free method.

The analysis by different methods indicate that coherent activity of the cortical and subcortical regions in the anticorrelated networks was markedly enhanced by acupuncture stimulation. This, in the context of the dysfunction of the DMN’s functional connectivity in

diseased states, may give us new insights into how acupuncture's generalized neurological effects correlate to its beneficial clinical effects.

4. Experimental Procedures

4.1. Participants

The study was performed at the Athinoula A Martinos Center for Biomedical Imaging, Department of Radiology, Massachusetts General Hospital in compliance with the Code of Ethics of the World Medical Association (Declaration of Helsinki) and the standards established by the Institutional Review Board of the hospital and the National Center of Complementary and Alternative Medicine (NCCAM) of the NIH. The subjects were screened to exclude neurological, mental and medical disorders, drug abuse, history of head trauma with loss of consciousness, and contraindications for exposure to high magnetic field. The nature of the experimental procedures was explained to the subjects, and signed informed consent form was obtained prior to participation in the study.

4.2 Features of experimental design

The study of acupuncture with fMRI is challenging due to low signal to noise ratios as well as high inter-subject and intersession variability (Kong et al., 2007, 2009). The use of small sample sizes has been a major limitation of past acupuncture studies. Our accumulative acupuncture data acquired with fMRI by the same protocol provides the largest sample size study with high statistical power that is most valuable in such investigation. Instead of using acupuncture at 'non-meridian' acupoints for control, we opted to use tactile stimulation over the acupoint as a form of conventional sensory stimulation for comparison to extract the response unique to acupuncture. The separation of subjects with inadvertent sharp pain during acupuncture from the major cohort who experienced *deqi* avoided the confounding effect of noxious stimulation which could account for discrepancies. The use of different acupoints on the same subjects in the same session minimized individual and intersession variability. Importantly. this is the first study that compares the networks involved during acupuncture stimulation with those of the intrinsic global networks of the resting brain.

4.3 Procedures

4.3.1 Acupuncture Stimulation—During fMRI scaning, acupuncture stimulation was administered in duplicate runs to classical acupoints on the right, LI4 on the hand, LV3 on the foot or ST36 on the lower leg in randomized order on each subject, employing sterile, one-time use only acupuncture needles. Stainless steel needles were used for LV3 (0.20 mm diameter) and ST36 (0.22 mm diameter) (KINGLI Medical Appliance Co. Wuxi, China); silver needles (0.23 mm diameter) were used for LI4 (Matsuka, Tokyo, Japan). The depth of needle insertion varied, ranging from 0.5-1 cm for the LV3 and LI4 to 2-3 cm for ST36 because of the nature of each acupoint. *Deqi* is a composite of unique sensations such as aching and soreness commonly associated with acupuncture and related to efficacy according to Traditional Chinese Medicine (TCM) (Hui et al., 2007). In order to evoke *deqi* and avoid noxious stimulation, the subject's sensitivity and tolerance to needle manipulation was tested after needle insertion prior to performing acupuncture with imaging. The results helped in choosing the depth of needle insertion and the force of needle manipulation to be used for data collection. During the 10 min scan, the needle was rotated approximately 180° in each direction with even motion at the rate of 1Hz for 2 min during two stimulation periods M1 and M2, and left in place during the three rest periods R1 (2 min), R2 (3 min) and R3 (1 min) (Fig 8). The needle was left in place at the end of the first scan when the subject was asked to score the sensations experienced during needle manipulation. This was followed by another 10 min acupuncture scan using the same paradigm. Thus the subject received a total of 8 min of enhanced acupuncture stimulation during a 20-25 min period. In

order to avoid excessive discomfort, the subject was instructed before scanning to raise one finger if any sensation during stimulation reached the intensity of 7-8 on a scale of 1-10 and raise 2 fingers in case of any sharp pain. When so signaled, the acupuncturist would immediately reduce the magnitude of needle rotation, and the excess discomfort would generally subside within a couple of seconds. A licensed acupuncturist (JL) in clinical practice for over 25 years administered the acupuncture for all the subjects.

4.3.2. Tactile Stimulation—Each subject received tactile stimulation as control before receiving the first acupuncture of the session while still naïve to the acupuncture sensations. The skin over the acupoint was tapped gently with a 5.88 von Frey monofilament using a matched paradigm. The participant was blinded to the study, being told that acupuncture was to be performed at different acupuncture points using different techniques, and the tests being performed could not be seen from the subject's supine position in the scanner. The procedure therefore also takes into account the effects of expectation and can be regarded as a form of 'sham acupuncture' (Napadow et al. 2007).

4.3.3 Interview for Psychophysical Response—At the completion of each acupuncture or tactile stimulation scan, the subject was asked to report if any of these sensations occurred during the procedure (aching, soreness, pressure, heaviness, fullness, warmth, coolness, numbness, tingling, dull pain, sharp pain) and to rate each sensation, if present, on a scale of 1-10 (Hui et al., 2007).

4.3.4 Functional MRI—Imaging of the brain was conducted on a 1.5 Tesla Siemens Sonata MRI system (Siemens, Erlangen, Germany) equipped for echo planar imaging with a standard quadratic head coil. The subjects lay supine wearing ear plugs to suppress scanner noise and with the head immobilized by cushioned supports. T1-weighted 3D MPRAGE (magnetization-prepared rapid acquisition gradient echo) anatomical images (128 images/set, TR/TE 2.73/3.39 ms, matrix 256×192, FOV 256 mm, flip angle 7°) were collected. Functional scans encompassing the whole brain including the brainstem were acquired with 38 sagittal slices parallel to the AC-PC plane using a T2*-weighted gradient echo sequence (TR/TE 4000/30 ms, FOV 200×200 mm, matrix 64×64, flip angle 90°, slice thickness 3.0 mm, gap 0.6 mm), giving a total of 150 time points in 10 min. Image collection was preceded by 4 dummy scans to allow for equilibration of the fMRI signal. The relatively long TR permits whole brain coverage with high spatial resolution. It has been shown that robust intrinsic correlations could be observed consistent with those using shorter repetition time (Kahn et al., 2008).

4.4. Data Analysis

4.4.1. Psychophysical Response—Analysis of the psychophysical response was described in previous reports (Hui et al., 2005, 2007). Briefly, the *deqi* response was defined as a total score of 3 or higher for the recorded sensations other than sharp pain. Any inadvertent sharp pain lasting more than 1 second was considered noxious stimulation. The subjects were grouped according to their psychophysical response: *deqi* (*deqi* only), *mixed* (*deqi* mixed with sharp pain) and *nil* (no specific sensations). None of the subjects experienced noxious stimulation without *deqi* sensations.

4.4.2. fMRI general linear model analysis—Results from each subject were analyzed individually to check for trends and anomalies. Duplicate runs of acupuncture or tactile stimulation on the acupoint of an individual associated with the same psychophysical response were averaged to provide data for group analysis. Signal intensities from rest periods with needles in place before and after each needle stimulation were taken as the baseline to assess the change in neurological BOLD signal induced by the needle

manipulation. Primary analysis was carried out using AFNI (Cox, 1996). The first 15 volumes collected in the first minute of each functional scan were discarded to allow the subject recover from possible effects of needle insertion and minimize the drift of signals in the baseline prior to active stimulation. The data-sets were transformed to a common three dimensional digital space, Talairach space (Talairach and Tournoux, 1988), normalized to average image intensity and blurred with a Gaussian kernel of full-width half-maximum (FWHM) value of 3 mm to account for any residual differences between runs. Functional data-sets showing a gross motion exceeding 2 mm on any axis were excluded from further analysis.

Time series statistical analysis was performed to find brain areas showing changes of MR signals during acupuncture or tactile stimulation with reference to the baseline using a general linear model of AFNI's 3dDeconvolve (Cox, 1996), which determines both the % signal change at each voxel as well as the statistical significance of the signal change across subjects. The significance level for group data was set at $p < 0.001$ ($t > 3.37$) and a minimum cluster size of 3 contiguous voxels (each measuring 3.125 × 3.125 × 3.6mm with a total volume of 105 mm^3). In order to address the multiple comparison correction, a Monte Carlo simulation was completed, the results of which demonstrated that such a combination of clustering and thresholding produced a false discovery rate α of less than 0.4% (AlphaSim, AFNI). The p-value maps were interpolated to 1mm using a cubic interpolation algorithm and overlaid on the high-resolution anatomical data of the cohort.

Brain volumes from 37 subjects were run through a paired, voxel by voxel, t-test with acupuncture and superficial tactile stimulation matched for acupoint to compare the change in signal intensity and the volume involved. Statistical p-maps were created for each of the contrasts of interest. Signal change during acupuncture and tactile stimulation were further analyzed to show the volume involved within important structures. Another random effects analysis, a standard voxel by voxel two sample t test (3dttest, AFNI), was performed to compare the hemodynamic response of *deqi* to mixed sensations.

4.4.3. Correlation analyses—We first analyzed the functional connectivity with the commonly used seed-based CCA which uses the average activity of a seed region (a sphere with radius 4.5mm) to find other voxels in the brain that behave similarly (Biswal et al., 1995; Fox et al., 2005; Vincent et al., 2006). Cross correlation analysis has the benefit of accounting for both delayed and residual effects of needle manipulation, as it is based on the seed's neurological time-course rather than that of our paradigm. We applied a band pass filter 0.003-0.08 Hz onto the preprocessed data (averages of duplicate runs by subject) to remove cardiac and respiratory signals at frequencies of >0.08 Hz and non-physiological noise at frequencies of <0.003 Hz in order to isolate the low frequency fluctuations characteristic of the resting brain for further analysis (3dFourier, AFNI). The signals found within the ventricles and within the white matter were regressed to remove regionally non-specific correlations that appear in every region of the brain (Biswal et al., 1995; Fox et al., 2005; Kahn et al., 2008; Vincent et al., 2006).

In the selection of regions of reference or seeds for CCA we focused on networks that overlapped with the DMN and limbic structures of special interest in acupuncture action. The pregenual cingulate, SG25, posterior cingulate BA31, hippocampus, amygdala, and hypothalamus on the right, ipsilateral to the site of stimulation, were selected for the deactivation network (Buckner et al., 2008; Fox et al., 2005; Fransson, 2005; Greicius et al., 2003; Lowe et al., 1998). In addition, the contralateral SII on the left and the right anterior insula were also selected as reference regions for CCA of the activation network. The objective is to explore how the insula, a paralimbic structure, may differ from a somatosensory structure in its functional connectivity with the rest of the brain although the

two are considered a part of the task-positive network in the literature (Fox et al., 2005; Fransson, 2005).

The average time-course of the voxels in a sphere of 4.5 mm radius around the maximal voxel in each region of reference was correlated (3dfim+, AFNI) with the measured fMRI time-course of each voxel for each scan (Fox, et al. 2005; Vincent, et al. 2006). The resultant statistical map of each correlation analysis was normalized to z-values using the Fisher's r-to-z transformation. The z-maps showed values for each voxel that were approximately normally distributed across subjects. These individual z-maps were compared with a t-test (3dttest, AFNI) to obtain t-maps representing regions statistically correlated with the seed across all subjects.

The functional connectivity obtained by seed-based CCA was cross-checked with probabilistic independent component analysis (pICA) by MELODIC (Multivariate Exploratory Linear Optimized Decomposition into Independent Components) (Beckmann and Smith, 2004, 2005). Because of the same limitation caused by global and external signals, the same data that had been run through a band pass filter of 0.003-0.08 Hz and a regression of the global signal for seed-based CCA was used for this method. Being data-driven, this method does not use paradigm, time series, or regions of reference to compile results, which will minimize inspector bias and accounts for temporally delayed as well as for residual effects. Therefore, the agreement between the results produced by different methods would strengthen the reliability of our findings.

For pICA, the data that had been run through the band pass filter and regressed was analyzed with the FSL MELODIC software (www.fmrib.ox.ac.uk/fsl/melodic/index.html) using its Tensorial Independent Component Analysis (TICA) function. This produces a set of independent components (spatio-temporal maps that are both uncorrelated and non-Gaussian) that designate general trends in neurological activity across major regions of the brain. The mixture model-based inference was set to a standard value of 0.5. We did not set a limit to the number of independent components as to avoid any potential bias of our results. The independent components, automatically created from the 4D data, are in the form of a Z statistic for which activated or deactivated areas may be considered temporally coherent. The Z-scores reflect the degree to which a given voxel's time series correlates with the overall component time series, which are scaled by residual Gaussian noise. This has the benefit of first cleaning non-useful signals, and showing maps of correlated areas, or areas in a general functional network. From the large number of components generated by the analysis, we selected the components that most closely matched the response described for the resting brain as well as the response we commonly observe during acupuncture stimulation. The time series of these components were compared with our experimental paradigm. The pICA method also has the advantage of being better able to remove low frequency fluctuations from physiological noise that may potentially contaminate seed-based CCA (Beckmann et al., 2005; Beckmann and Smith, 2004; Birn et al., 2006). It is one of the more concurrent commonly used model-free methods for functional connectivity in fMRI studies (Greicius et al., 2007; Levan and Gotman, 2008; Rombouts et al., 2007).

4.4.4. Anatomical localizations—Most anatomical definitions of the regions of interest were based on methods previously published through the Center for Morphometric Analysis, Department of Neurology, MGH (Caviness et al., 1996; Filipek et al., 1994), and multiple standard atlases such as Talairach (Talairach and Tournoux, 1988) and Mai (Mai et al., 2004). Subdivisions of the cingulate were based on Vogt's studies (Vogt, 2005; Vogt et al., 2003, 2006). The anatomical localization and labeling of the functional data were determined both by Talaraich coordinates and direct inspection.

Supplementary Material

Refer to Web version on PubMed Central for supplementary material.

Acknowledgments

The work was supported in part by the NIH/National Center for Complementary and Alternative Medicine (R21AT00978) (1-P01-002048-01) (K01-AT-002166-01), the National Center for Research Resources (P41RR14075), the Mental Illness and Neuroscience Discovery Institute and the Brain Project Grant NS 34189. We thank Randy L. Buckner and Moshe Bar for insightful comments and advice and Justin L. Vincent for valuable suggestions on data analysis.

Abbreviations

AFNI	analysis for neuroimaging
Amy	amygdala
BA23d	BA23dorsal
BA23v	BA23ventral
BOLD	blood oxygenation level-dependent
CCA	cross correlation analysis
DLPFC	dorsolateral prefrontal cortex
DMN	default mode network
DMPFC	dorsomedial prefrontal cortex
FP	frontal pole
GLM	general linear model
Hpc	hippocampus
Hpc+	hippocampal formation
Hypo	hypothalamus
LPNN	limbic-paralimbic-neocortical network
MELODIC	Multivariate Exploratory Linear Optimized Decomposition into Independent Components
midC	middle cingulate
MPC	medial parietal cortex
MPFC	medial prefrontal cortex
MTL	medial temporal lobe
OFC	orbitofrontal cortex
PCN	precuneus
PHpc	parahipocampus
pICA	probabilistic independent component analysis
pregC	pregenual cingulate
postC	posterior cingulate
ROI	region of interest

RSC	retrosplenial, cortex
SII	secondary somatosensory cortex
subgC	subgenual cingulate
SG25	subgenual area 25
TCM	traditional Chinese medicine
TP	temporal pole
VMPFC	ventromedial prefrontal cortex

REFERENCES

Anand A, Li Y, Wang Y, Gardner K, Lowe MJ. Reciprocal effects of antidepressant treatment on activity and connectivity of the mood regulating circuit: an FMRI study. J Neuropsychiatry Clin Neurosci. 2007; 19(3):274–82. [PubMed: 17827412]

Apkarian AV, Bushnell MC, Treede Rolf-Detlef, Zubieta Jon-Kar. Human brain mechanisms of pain perception and regulation in health and disease. Eur J Pain. 2005; 9:463–484. [PubMed: 15979027]

Beckmann CF, DeLuca M, Devlin JT, Smith SM. Investigations into resting-state connectivity using independent component analysis. Philos Trans R Soc Lond B Biol Sci. 2005; 360(1457):1001–13. [PubMed: 16087444]

Beckmann CF, Smith SM. Probabilistic independent component analysis for functional magnetic resonance imaging. IEEE Trans Med Imaging. 2004; 23(2):137–52. [PubMed: 14964560]

Beckmann CF, Smith SM. Tensorial extensions of independent component analysis for multisubject FMRI analysis. Neuroimage. 2005; 25(1):294–311. [PubMed: 15734364]

Binder JR, Frost JA, Hammeke TA, Bellgowan PS, Rao SM, Cox RW. Conceptual processing during the conscious resting state. A functional MRI study. J Cogn Neurosci. 1999; 11(1):80–95. [PubMed: 9950716]

Birn RM, Diamond JB, Smith MA, Bandettini PA. Separating respiratory-variation related fluctuations from neuronal-activity-related fluctuations in fMRI. Neuroimage. 2006; 31(4):1536–48. [PubMed: 16632379]

Biswal B, Yetkin FZ, Haughton VM, Hyde JS. Functional connectivity in the motor cortex of resting human brain using echo-planar MRI. Magn Reson Med. 1995; 34(4):537–41. [PubMed: 8524021]

Bluhm RL, Miller J, Lanius RA, Osuch EA, Boksman K, Neufeld RW, Theberge J, Schaefer B, Williamson P. Spontaneous low-frequency fluctuations in the BOLD signal in schizophrenic patients: anomalies in the default network. Schizophr Bull. 2007; 33(4):1004–12. [PubMed: 17556752]

Buckner RL, Andrews-Hanna JR, Schachter DL. The brain's default network: Anatomy, function, and relevance to disease. Annals of the New York Academy of Sciences. 2008; 1124:1–38. [PubMed: 18400922]

Cao Q, Zang Y, Sun L, Sui M, Long X, Zou Q, Wang Y. Abnormal neural activity in children with attention deficit hyperactivity disorder: a resting-state functional magnetic resonance imaging study. Neuroreport. 2006; 17(10):1033–6. [PubMed: 16791098]

Castellanos FX, Margulies DS, Kelly C, Uddin LQ, Ghaffari M, Kirsch A, Shaw D, Shehzad Z, Di Martino A, Biswal B. Cingulate-precuneus interactions: a new locus of dysfunction in adult attention-deficit/hyperactivity disorder. Biol Psychiatry. 2008; 63(3):332–7. others. [PubMed: 17888409]

Caviness V, Meyer J, Makris N, Kennedy D. MRI-based topographic parcellation of human neocortex: an anatomically specified method with estimate reliability. Journal of Cognitive Neuroscience. 1996; 8:566–587.

Cheng, XN. Chinese Acupuncture and Moxibustion. People's Medical Publishing House; Beijing: 2000.

Corbetta M, Shulman GL. Control of goal-directed and stimulus-driven attention in the brain. Nat Rev Neurosci. 2002; 3(3):201–15. [PubMed: 11994752]

Cox RW. AFNI: software for analysis and visualization of functional magnetic resonance neuroimages. Comput Biomed Res. 1996; 29(3):162–73. [PubMed: 8812068]

Dhond RP, Yeh C, Park K, Kettner N, Napadow V. Acupuncture modulates resting state connectivity in default and sensorimotor brain networks. Pain. Jun; 2008 136(3):407–18. [PubMed: 18337009]

Dincer F, Linde K. Sham interventions in randomized clinical trials of acupuncture--A review. Complement Ther Med. 2003; 11(4):235–42. [PubMed: 15022656]

Drevets WC. Orbitofrontal cortex function and structure in depression. Ann N Y Acad Sci. 2007; 1121:499–527. [PubMed: 17872395]

Fang J, Zhen J, Li K, Kong J, Nixon E, Zeng Y, Tong H, Wang P, Hui KKS. The salient characteristics of the central effects of acupuncture needling: limbic-paralimbic-neocortical network modulation. Hum Brain Mapp. Jun 20; 2008 30(4):1196–1206. Epub ahead of print. [PubMed: 18571795]

Fang SH, Zhang SC, Liu HB. Study on brain responses to acupuncture by functional nuclear magnetic resonance - observations on 10 healthy subjects. Zhongguo zhong xi yi ze he za zhi. 2006; 26(14): 965–8.

Filipek PA, Richelme C, Kennedy DN, Caviness VS Jr. The young adult human brain: an MRI-based morphometric analysis. Cereb Cortex. 1994; 4(4):344–60. [PubMed: 7950308]

Fox MD, Snyder AZ, Vincent JL, Corbetta M, Van Essen DC, Raichle ME. The human brain is intrinsically organized into dynamic, anticorrelated functional networks. Proc Natl Acad Sci U S A. 2005; 102(27):9673–8. [PubMed: 15976020]

Fransson P. Spontaneous low-frequency BOLD signal fluctuations: an fMRI investigation of the resting-state default mode of brain function hypothesis. Hum Brain Mapp. 2005; 26(1):15–29. [PubMed: 15852468]

Fujiwara S, Sasaki M, Kanbara Y, Inoue T, Hirooka R, Ogawa A. Feasibility of 1.6-mm isotropic voxel diffusion tensor tractography in depicting limbic fibers. Neuroradiology. 2008; 50(2):131–6. [PubMed: 17938897]

Golland Y, Golland P, Bentin S, Malach R. Data-driven clustering reveals a fundamental subdivision of the human cortex into two global systems. Neuropsychologia. 2008; 46(2):540–53. [PubMed: 18037453]

Greicius MD, Flores BH, Menon V, Glover GH, Solvason HB, Kenna H, Reiss AL, Schatzberg AF. Resting-State Functional Connectivity in Major Depression: Abnormally Increased Contributions from Subgenual Cingulate Cortex and Thalamus. Biol Psychiatry. Sep; 2007 62(5):429–37. [PubMed: 17210143]

Greicius MD, Krasnow B, Reiss AL, Menon V. Functional connectivity in the resting brain: a network analysis of the default mode hypothesis. Proc Natl Acad Sci U S A. 2003; 100(1):253–8. [PubMed: 12506194]

Greicius MD, Menon V. Default-mode activity during a passive sensory task: uncoupled from deactivation but impacting activation. J Cogn Neurosci. 2004; 16(9):1484–92. [PubMed: 15601513]

Greicius MD, Supekar K, Menon V, Dougherty RF. Resting-State Functional Connectivity Reflects Structural Connectivity in the Default Mode Network. Cereb Cortex. Jan; 2009 19(1):72–8. [PubMed: 18403396]

Gusnard DA, Raichle ME. Searching for a baseline: functional imaging and the resting human brain. Nat Rev Neurosci. 2001; 2(10):685–94. [PubMed: 11584306]

Han JS. Acupuncture: neuropeptide release produced by electrical stimulation of different frequencies. Trends Neurosci. 2003; 26(1)

He Y, Wang L, Zang Y, Tian L, Zhang X, Li K, Jiang T. Regional coherence changes in the early stages of Alzheimer's disease: a combined structural and resting-state functional MRI study. Neuroimage. 2007; 35(2):488–500. [PubMed: 17254803]

Ho TJ, Duann JR, Chen CM, Chen JH, Shen WC, Lu TW, Liao JR, Lin JG. Carryover effects alter FMRI statistical analysis in an acupuncture study. Am J Chin Med. 2008; 36(1):55–70. [PubMed: 18306450]

Hollifield M, Sinclair-Lian N, Warner TD, Hammerschlag R. Acupuncture for post-traumatic stress disorder: a randomized controlled pilot trial. J Nerv Ment Dis. 2007; 195(6):504–13. [PubMed: 17568299]

Honey CJ, Sporns O, Cammoun L, Gigandet X, Thiran JP, Meuli R, Hagmann P. Predicting human resting-state functional connectivity from structural connectivity. Proc Natl Acad Sci U.S.A. 2009; 106(6):2035–40. [PubMed: 19188601]

Hua QP, Zeng XZ, Liu JY, Wang JY, Gao JY, Luo F. Dynamic changes in Brain activation and functional connectivity during affectively different tactile stimuli. Cell Mol Neurobiol. 2008; 2008; 28:57–70. [PubMed: 18000754]

Hui KK, Liu J, Makris N, Gollub RL, Chen AJ, Moore CI, Kennedy DN, Rosen BR, Kwong KK. Acupuncture modulates the limbic system and subcortical gray structures of the human brain: evidence from fMRI studies in normal subjects. Hum Brain Mapp. 2000; 9(1):13–25. [PubMed: 10643726]

Hui KK, Liu J, Marina O, Napadow V, Haselgrove C, Kwong KK, Kennedy DN, Makris N. The integrated response of the human cerebro-cerebellar and limbic systems to acupuncture stimulation at ST 36 as evidenced by fMRI. Neuroimage. 2005; 27(3):479–96. [PubMed: 16046146]

Hui KK, Nixon EE, Vangel MG, Liu J, Marina O, Napadow V, Hodge SM, Rosen BR, Makris N, Kennedy DN. Characterization of the "*Deqi*" Response in Acupuncture. BMC Complement Altern Med. 2007; 7(1):33. [PubMed: 17973984]

Hui KKS, Liu J, Rosen BR, Kwong KK. Effects of acupuncture on the human limbic system and basal ganglia measured by fMRI. Proc. 3rd Intl Conference on Functional Mapping of the Human Brain. NeuroImage. 1997; 5(4):S226.

Kahn I, Andrews-Hanna JR, Vincent JL, Snyder AZ, Buckner RL. Distinct cortical anatomy linked to subregions of the medial temporal lobe revealed by intrinsic functional connectivity. J Neurophysiol. 2008; 100(1):129–39. [PubMed: 18385483]

Kennedy DP, Courchesne E. The intrinsic functional organization of the brain is altered in autism. Neuroimage. 2008; 39(4):1877–85. [PubMed: 18083565]

Kennedy DP, Redcay E, Courchesne E. Failing to deactivate:resting functional abnormalities in autism. Proc Natl Acad Sci U S A. 2006; 103(21):8275–80. [PubMed: 16702548]

Kong J, Gollub R, Webb JM, Kong JT, Vangel MG, Kwong K. Test test-retest study of fMRI signal change evoked by electroacupuncture stimulation. Neuroimage. 2007; 34:1171–1181. [PubMed: 17157035]

Kong J, Kaptchuk TJ, Webb JM, Kong JT, Sasaki Y, Polich G, Vangel MG, Kwong K, Rosen B, Gollub RL. Functional neuroanatomical investigation of vision-related acupuncture point specificity – a multisession fMRI study. Hum Brain Mapp. 2009; 30:38–46. [PubMed: 17990299]

Leo RJ, Ligot JS Jr. A systematic review of randomized controlled trials of acupuncture in the treatment of depression. J Affect Disord. 2007; 97(1-3):3–22.

Levan P, Gotman J. Independent component analysis as a model-free approach for the detection of BOLD changes related to epileptic spikes: A simulation study. Hum Brain Mapp. Aug 22.2008 Epub ahead of print PMID 18726909.

Liang M, Zhou Y, Jiang T, Liu Z, Tian L, Liu H, Hao Y. Widespread functional disconnectivity in schizophrenia with resting-state functional magnetic resonance imaging. Neuroreport. 2006; 17(2): 209–13. [PubMed: 16407773]

Liu S, Zhou W, Ruan X, Li R, Lee T, Weng X, Hu J, Yang G. Activation of the hypothalamus characterizes the response to acupuncture stimulation in heroin addicts. Neurosci Lett. 2007; 421(3):203–8. [PubMed: 17574746]

Lowe MJ, Mock BJ, Sorenson JA. Functional connectivity in single and multislice echoplanar imaging using resting-state fluctuations. Neuroimage. 1998; 7(2):119–32. [PubMed: 9558644]

Lowe MJ, Phillips MD, Lurito JT, Mattson D, Dzemidzic M, Mathews VP. Multiple sclerosis: low-frequency temporal blood oxygen level-dependent fluctuations indicate reduced functional connectivity initial results. Radiology. 2002; 224(1):184–92. [PubMed: 12091681]

Lund I, Lundeberg T. Are minimal, superficial or sham acupuncture procedures acceptable as inert placebo controls? Acupunct Med. 2006; 24(1):13–5. [PubMed: 16618044]

Lustig C, Snyder AZ, Bhakta M, O'Brien KC, McAvoy M, Raichle ME, Morris JC, Buckner RL. Functional deactivations: change with age and dementia of the Alzheimer type. Proc Natl Acad Sci U S A. 2003; 100(24):14504–9. [PubMed: 14608034]

Mai, JK.; Assheur, J.; George, P. Atlas of the Human Brain. Second Edition. Elsevier Academic Press; London: 2005.

Mayberg HS. Modulating dysfunctional limbic-cortical circuits in depression: towards development of brain-based algorithms for diagnosis and optimized treatment. Br Med Bull. 2003; 65:193–207. [PubMed: 12697626]

Mayberg HS. Defining the neural circuitry of depression: toward a new nosology with therapeutic implications. Biol Psychiatry. 2007; 61(6):729–30. [PubMed: 17338903]

Mori S, van Zijl P. Human white matter atlas. Am J Psychiatry. 2007; 164(7):1005. [PubMed: 17606649]

Napadow V, Kettner N, Liu J, Li M, Kwong KK, Vangel M, Makris N, Audette J, Hui KK. Hypothalamus and amygdala response to acupuncture stimuli in Carpal Tunnel Syndrome. Pain. 2007; 130(3):254–66. [PubMed: 17240066]

Napadow V, Makris N, Liu J, Kettner NW, Kwong KK, Hui KK. Effects of electro-acupuncture versus manual acupuncture on the human brain as measured by fMRI. Hum Brain Mapp. 2005; 24(3): 193–205. [PubMed: 15499576]

Napadow V, Liu J, Kaptchuk T. A systematic study of acupuncture practice: acupoint usage in an outpatient setting in Beijing, China. Complement Ther Med. 2004; 12(4):209–16. [PubMed: 15649834]

Olson IR, Plotzker A, Ezzyat Y. The Enigmatic temporal pole: a review of findings on social and emotional processing. Brain. 2007; 130(Pt7):1718–31. [PubMed: 17392317]

Parvizi J, Van Hoesen GW, Buckwalter J, Damasio A. Neural connections of the posteromedial cortex in the macaque. Proc Natl Acad Sci U S A. 2006; 103(5):1563–8. [PubMed: 16432221]

Rombouts SA, Barkhof F, Goekoop R, Stam CJ, Sheltens P. Altered resting staste networks in mild cognitive impairment and mild Alzheimer's disease: an fMRI study. Hum Brain Mapp. 2005; 26(4):231–9. [PubMed: 15954139]

Rombouts SA, Scheltens P, Kuijer JP, Barkhof F. Whole brain analysis of T2* weighted baseline FMRI signal in dementia. Hum Brain Mapp. 2007; 24(12):1313–7. [PubMed: 17290368]

Schmahmann, JD.; Pandya, DN. Fiber Pathways of the Brain. Oxford University Press; Oxford: 2006.

Schmahmann JD, Pandya DN, Wang R, Dai G, D'Arceuil HE, de Crespigny AJ, Wedeen VJ. Association fiber pathways of the brain: parallel observations from diffusion spectrum imaging and autoradiography. Brain. 2007; 130(Pt 3):630–53. [PubMed: 17293361]

Shulman GL, Corbetta M, Buckner RL, Raichle ME, Fiez JA, Miezin FM, Petersen SE. Top-down modulation of early sensory cortex. Cereb Cortex. 1997; 7(3):193–206. [PubMed: 9143441]

Stam R. PTSD and stress sensitisation: a tale of brain and body Part 1: human studies. Neurosci Biobehav Rev. 2007; 31(4):530–57. [PubMed: 17270271]

Stoffers D, Bosboom JL, Deijen JB, Wolters EC, Berendse HW, Stam CJ. Slowing of oscillatory brain activity is a stable characteristic of Parkinson's disease without dementia. Brain. 2007; 130(Pt 7): 1847–60. [PubMed: 17412733]

Talairach, J.; Tournoux, P. Co-planar stereotaxic atlas of the human brain: 3-Dimensional proportional system: an approach to medical cerebral imaging. Thieme Medical Pub; New York: 1988.

Tsukayama H, Kimura T, Otsuki K. Factors that influence the applicability of sham needle in acupuncture trials: two randomized, single-blind, crossover trials with acupuncture-experienced subjects. Clin J Pain. 2006; 22(4):346–9. [PubMed: 16691086]

Uddin LQ, Clare Kelly AM, Biswal BB, Xavier Castellanos F, Milham MP. Functional connectivity of default mode network components: Correlation, anticorrelation, and causality. Hum Brain Mapp. Jan 26.2008 2008 ISSN 1065-9471.

Vincent JL, Snyder AZ, Fox MD, Shannon BJ, Andrews JR, Raichle ME, Buckner RL. Coherent spontaneous activity identifies a hippocampal-parietal memory network. J Neurophysiol. 2006; 96(6):3517–31. [PubMed: 16899645]

Vogt BA. Pain and emotion interactions in subregions of the cingulate gyrus. Nat Rev Neurosci. 2005; 6(7):533–44. [PubMed: 15995724]

Vogt BA, Berger GR, Derbyshire SW. Structural and functional dichotomy of human mid-cingulate cortex. Eur J Neurosci. 2003; 18(11):3134–44. [PubMed: 14656310]

Vogt BA, Vogt L, Laureys S. Cytology and functionally correlated circuits of human posterior cingulate areas. Neuroimage. 2006; 29(2):452–66. [PubMed: 16140550]

Wang L, Zang Y, He Y, Liang M, Zhang X, Tian L, Wu T, Jiang T, Li K. Changes in hippocampal connectivity in the early stages of Alzheimer's disease: evidence from resting state fMRI. Neuroimage. 2006; 31(2):496–504. [PubMed: 16473024]

Wang W, Liu L, Zhi X, Huang JB, Liu DX, Wang H, Kong XQ, Xu HB. Study on the regulatory effect of electro-acupuncture on hegu point (LI4) in cerebral response with functional magnetic resonance imaging. Chin J Integ Med. 2007; 13(1):10–6.

White P, Lewith G, Hopwood V, Prescott P. The placebo needle, it ita valid and convincing placebo for use in acupuncture trials? A randomized, singl-blind, corss-over pilot try Pin. 2003; 106(3): 401–9.

White A, Cummings M, Barlas P, Cardini F, Filshie J, Foster NE, Lundeberg T, Stener-Victorin E, Witt C. Defining an adequate dose of acupuncture using a neurophysiological approach - a narrative review of the literature. Acupunct Med. 2008; 26(2):111–20. [PubMed: 18591910]

Willis, WD. The origin and destination of pathways involved in pain transmission. In: Melzack, R.; Wall, PD., editors. Textbook of Pain. 2nd ed. Churchill Livingstone; Edinburgh: 1989. p. 112-127.

Willis WD, Westlund KN. Neuroanatomy of the pain system and of the pathways that modulate pain. J Clin Neurophysiol. 1997; 14(1):2–31. [PubMed: 9013357]

Wu MT, Hsieh JC, Xiong J, Yang CF, Pan HB, Chen YC, Tsai G, Rosen BR, Kwong KK. Central nervous pathway for acupuncture stimulation: localization of processing with functional MR imaging of the brain--preliminary experience. Radiology. 1999; 212(1):133–41. [PubMed: 10405732]

Zang YF, He Y, Zhu CZ, Cao QJ, Sui MQ, Liang M, Tian LX, Jiang TZ, Wang YF. Altered baseline brain activity in children with ADHD revealed by resting-state functional MRI. Brain Dev. 2007; 29(2):83–91. [PubMed: 16919409]

Zhou Y, Liang M, Jiang T, Tian L, Liu Y, Liu Z, Liu H, Kuang F. Functional dysconnectivity of the dorsolateral prefrontal cortex in first-episode schizophrenia using resting-state fMRI. Neurosci Lett. 2007; 417(3):297–302. [PubMed: 17399900]

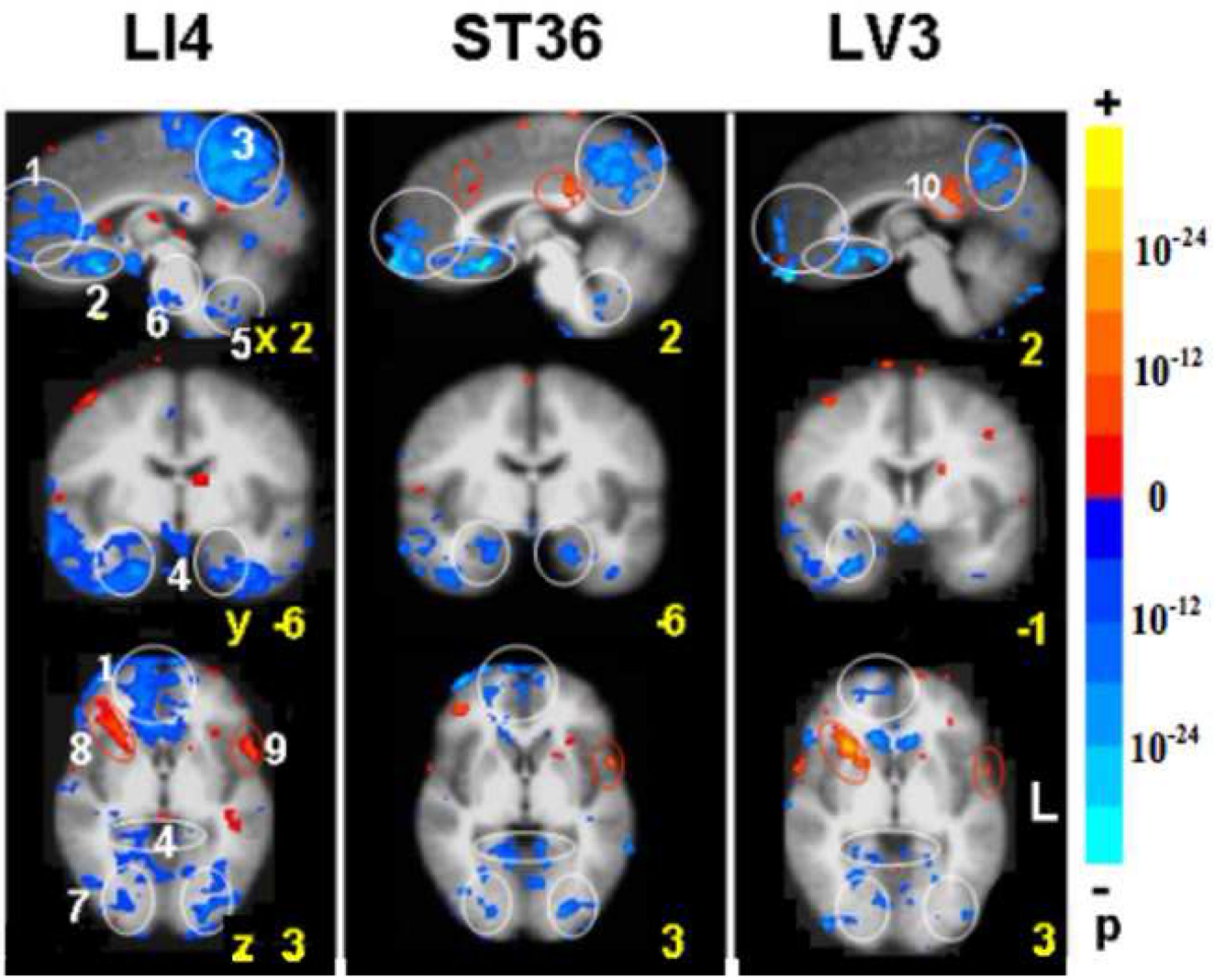

Fig. 1.

BOLD fMRI during acupuncture at 3 acupoints performed in randomized order (LI4 64 runs/37subjects, ST36 74/43, LV3 63/37). Clusters of deactivated regions appeared at the mid and ventral levels of the MPFC (1, 2), MPC (3) and MTL (4). Deactivation also occurred in the cerebellar tonsil and vermis (5), pontine nucleus (6) and extrastriate cortex (7). The general pattern was similar for all points with differences in magnitude of signal change and preferential localizations. Robust changes in all the regions were seen with LI4. Deactivation of the FP, pregC and cerebellum was minimal with LV3. A few paralimbic regions showed activation instead: the right anterior insula (8) and the postC-BA23d (9) with LI4 and LV3. The superior temporal gyrus BA22 (10) showed activation with all points. $p < 0.0001$

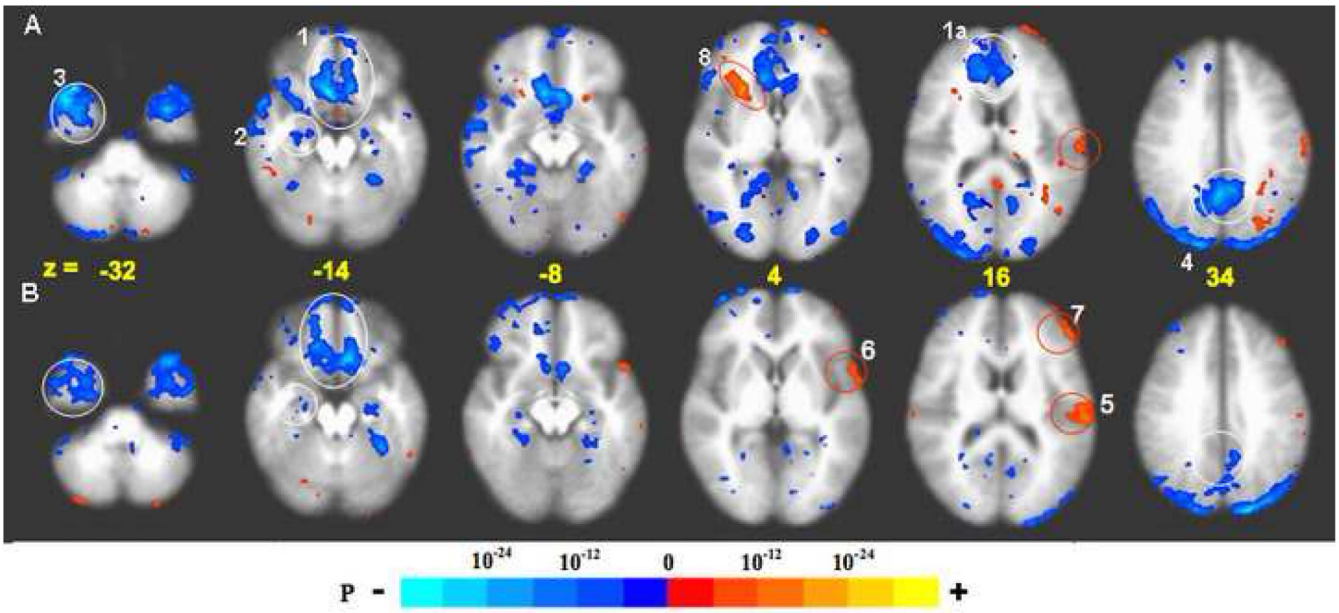

Fig. 2.

BOLD response: acupuncture *vs.* tactile stimulation at the right LI4, ST36, and LV3 acupoints performed on the same 37 subjects, $p < 0.001$. Deactivation network: In acupuncture (A) extensive deactivation appeared in the MPFC (1), MTL (2), TP (3) and MPC (4) regions. In tactile stimulation (B), deactivation appeared in similar regions but was more limited in extent than in acupuncture. The difference was most marked with the FP and pregC (1a) and PCN/BA31 (4). Activation network: Activation of SII (5), BA22 (6) and DLPFC (7) was more prominent in tactile stimulation than in acupuncture. The right anterior insula (8) notably showed strong activation with acupuncture but not with tactile stimulation (For details, see also Table 1).

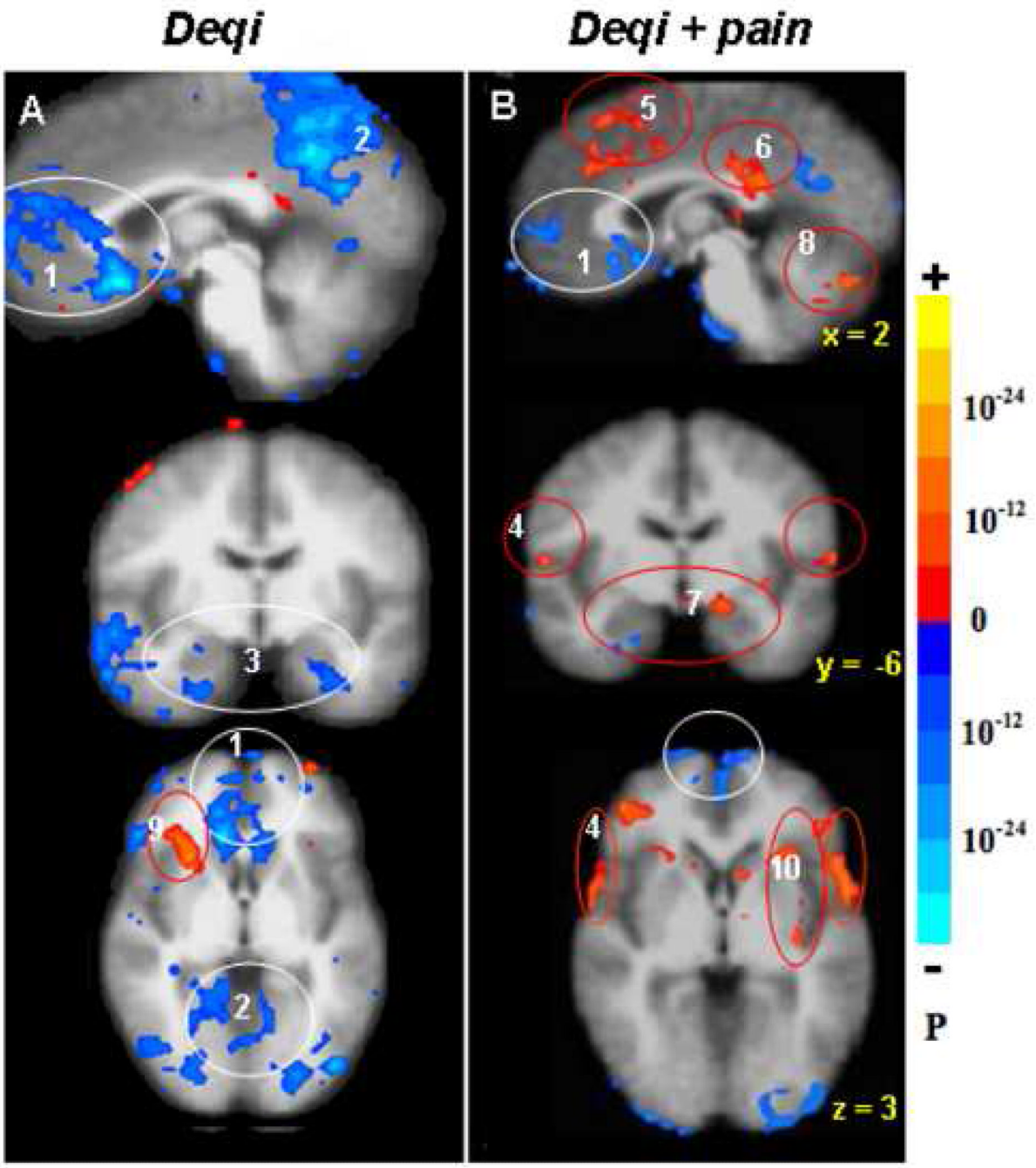

Fig. 3.

Distinct patterns of hemodynamic response between *deqi* (52 runs /37 subjects, A) and *deqi* mixed with sharp pain (52 runs/29 subjects, B) during acupuncture at right LI4, ST36 or LV3, $p < 0.0001$. The deactivation of the MPFC (1), MPC (2) and MTL (3) seen with *deqi* absent pain was attenuated in the presence of pain. With pain, activation of the sensorimotor and association cortices (4) became more prominent, and a subset of the limbic and paralimbic regions such as the midC/SMA (5), postC_BA23 (6), Amy (7), and cerebellar vermis (8) became activated. The right anterior insula (9) was markedly activated in *deqi* while smaller areas of anterior and posterior insula (10) were activated bilaterally in pain.

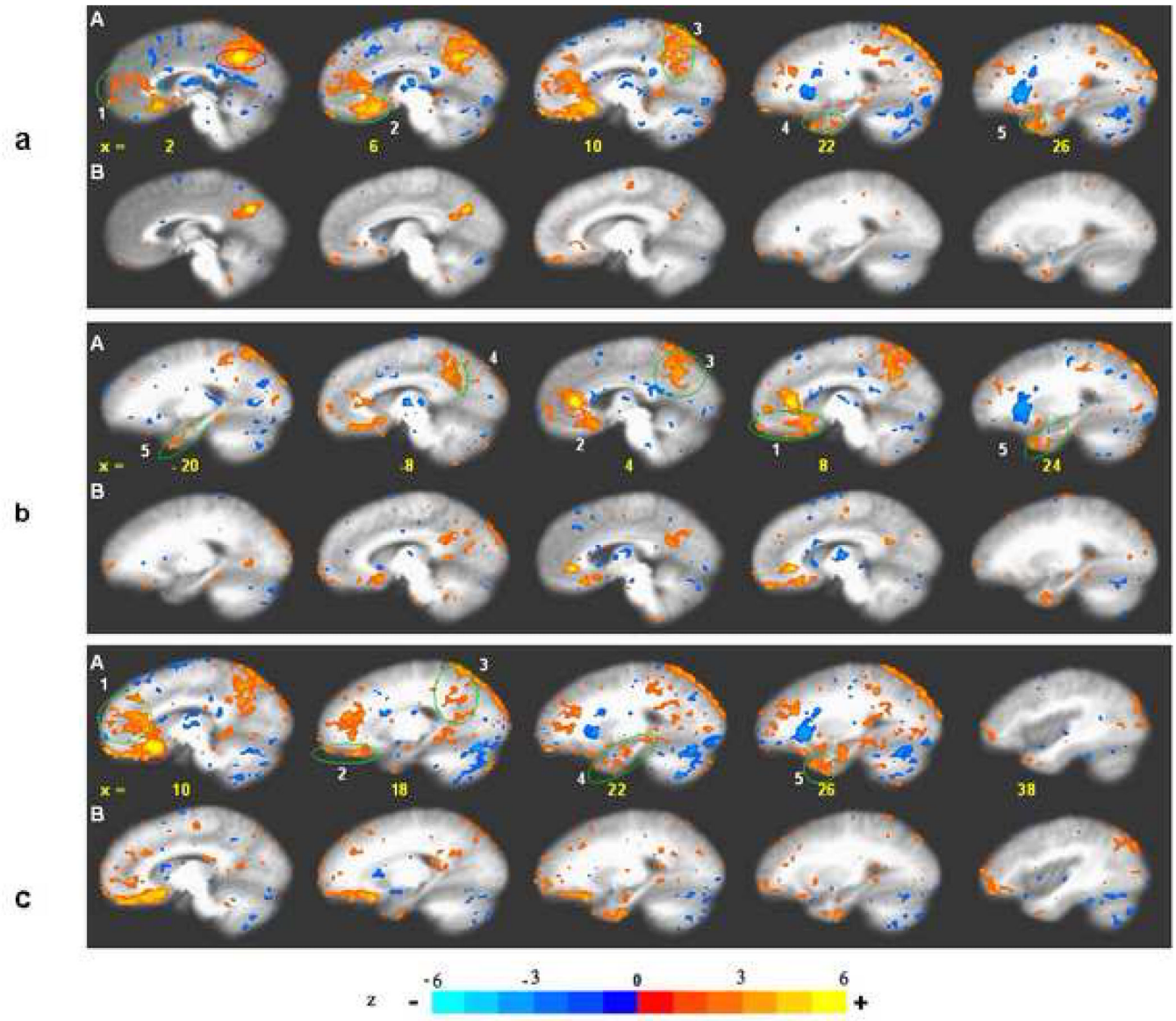

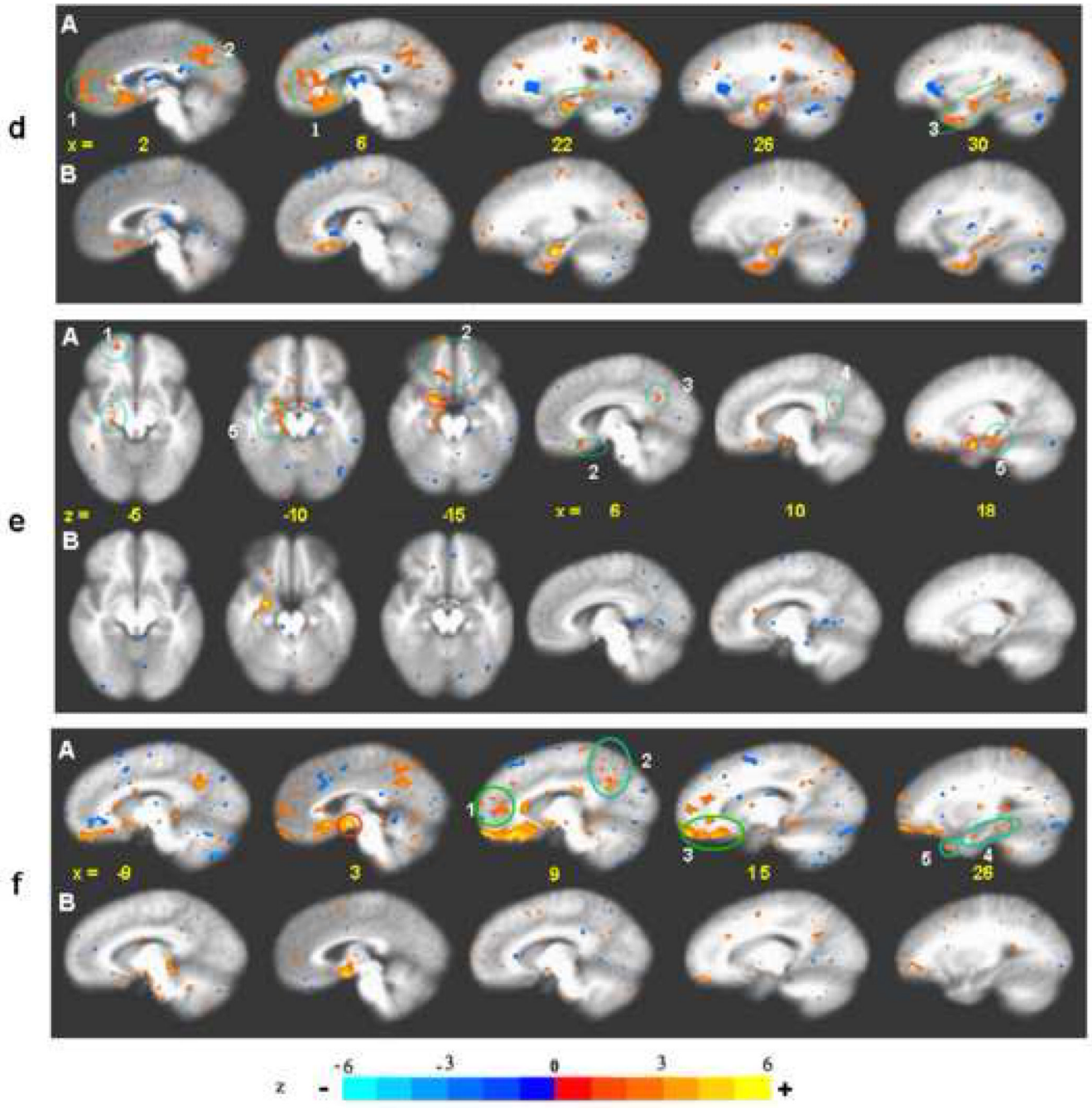

Fig. 4.1.

CCA deactivation network for acupuncture and tactile stimulation, Reference voxels are circled in red, and correlations are circled in green. $p < 0.001$

a) postC_BA31, right. Figure A. Acupuncture: Ref. voxel (2, −53, 36). There is extensive coherent deactivation bilaterally in the FP, pregC (l), OFC, subgC, SG25 (2) of the MPFC, the PCN, postC_BA31, 23v, RSC (3) of the MPC, the Amy, Hpc, PHpc (4) of the MTL and the TP (5). Figure B. Tactile Stimulation: Ref. voxel (3, −63, 31) Correlation regions overlap with those in acupuncture, but markedly weaker and more limited in extent.

b) PregC, right. Figure A. Acupuncture: Ref. voxel (5, 34, 9) Moderate correlations with BA10 (1), VMPFC, SG25 (2); PCN, BA 31(3), RSC (4) and MTL (5) were found. Figure B.

Tactile Stimulation: Ref. vox. (5, 34, −2) A similar spatial distribution but much weaker correlation than in acupuncture was found. There is insignificant correlation within pregC region and FP in midlevel MPFC; stronger correlation is found with VMPFC and subgenual areas in ventral route.

c) SG25, right. Figure A. Acupuncture: Ref. voxel: (5, 17, −13) Strong correlations are found with MPFC, more extensive in the dorsal (1) than in the ventral division (2) Also strong correlations are found with PMPC (3), MTL (4), and TP (5). Figure B. Tactile Stimulation: Ref. voxel (5, 14, −12) Correlations are seen with similar regions but weaker than in acupuncture. SG25 shows the strongest functional connectivity among the regions tested for the deactivation network in tactile stimulation.

d) Hpc, right. Figure A. Acupuncture: Ref. voxel (25, −11, −16). Correlations with MPFC (1), MPC (2) and other TL structures (3) are more limited in extent than with the use of other reference regions from the MPFC or MPC. Figure B. Tactile stimulation: Ref. voxel: (23, −10, −19) Correlations are found in similar regions as in acupuncture, but markedly reduced in extent with only focal correlation in MPC.

e) Amy, right. Figure A. Acupuncture: Ref. voxel (20, 2, −16). Correlations are seen with the FP (1), VMPFC (2), PCN/postC_BA31 of the MPC (3), RSC (4), Hpc/PHpc (5). Figure B. Tactile Stimulation: No significant signal change or regional correlations were found.

f) Hypothalamus, right. Figure A. Acupuncture: Ref. voxel (3, −1, −10) Correlations are seen with the FP, pregC (1), PCN, PCC (2) subgC, VMPFC, SG25 (3), Amy, Hpc, PHpc, TP (4) Figure B. Tactile Stimulation: Ref voxel (3, −1, −10) No significant signal change or regional correlations were found.

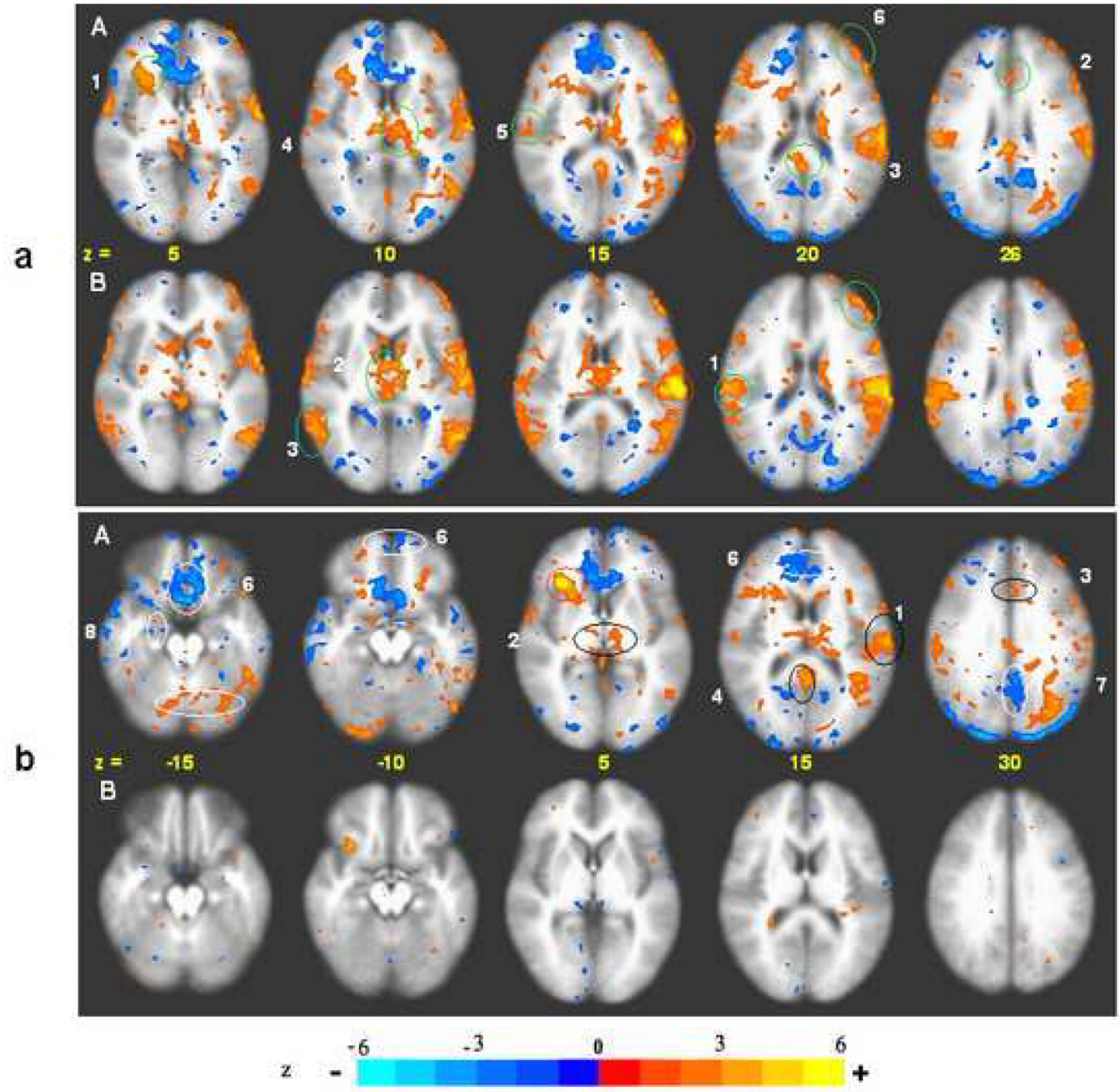

Fig. 4.2.

CCA: Acupuncture vs. tactile stimulation, Activation network. $p < 0.001$

a) SII, left (contralateral) Figure A. Acupuncture: Ref. voxel (−59, −20, 17). Correlations are seen with the right anterior insula (1), ant-midC (2). postC_BA23d (3), thalamus (4), ipsilateral SII (5), DLPFC_BA46 (6). Figure B. Tactile stimulation: Ref. voxel (−59, −21, 16). Correlations are seen with ipsilateral SII (1), thalamus (2), lateral temporal association cortex (3), DLPFC BA46 (4), stronger than in acupuncture, but no significant correlation with right anterior insula and midC.

b) Anterior Insula, right. Figure A. Acupuncture: Ref voxel (32, 26, 6). Positive correlations (circled in black) are seen with SII (1), thalamus (2), midC (3), postC_BA23 (4), BA22 (5).

Negative correlations (circled in white) are seen with MPFC (BA10/32/24/11/25) (6), MPC (BA31/7) (7), MTL (Hpc, PHpc) (8). Figure B. Tactile stimulation: Ref voxel (32, 26, 6). No significant signal change or regional correlations were found.

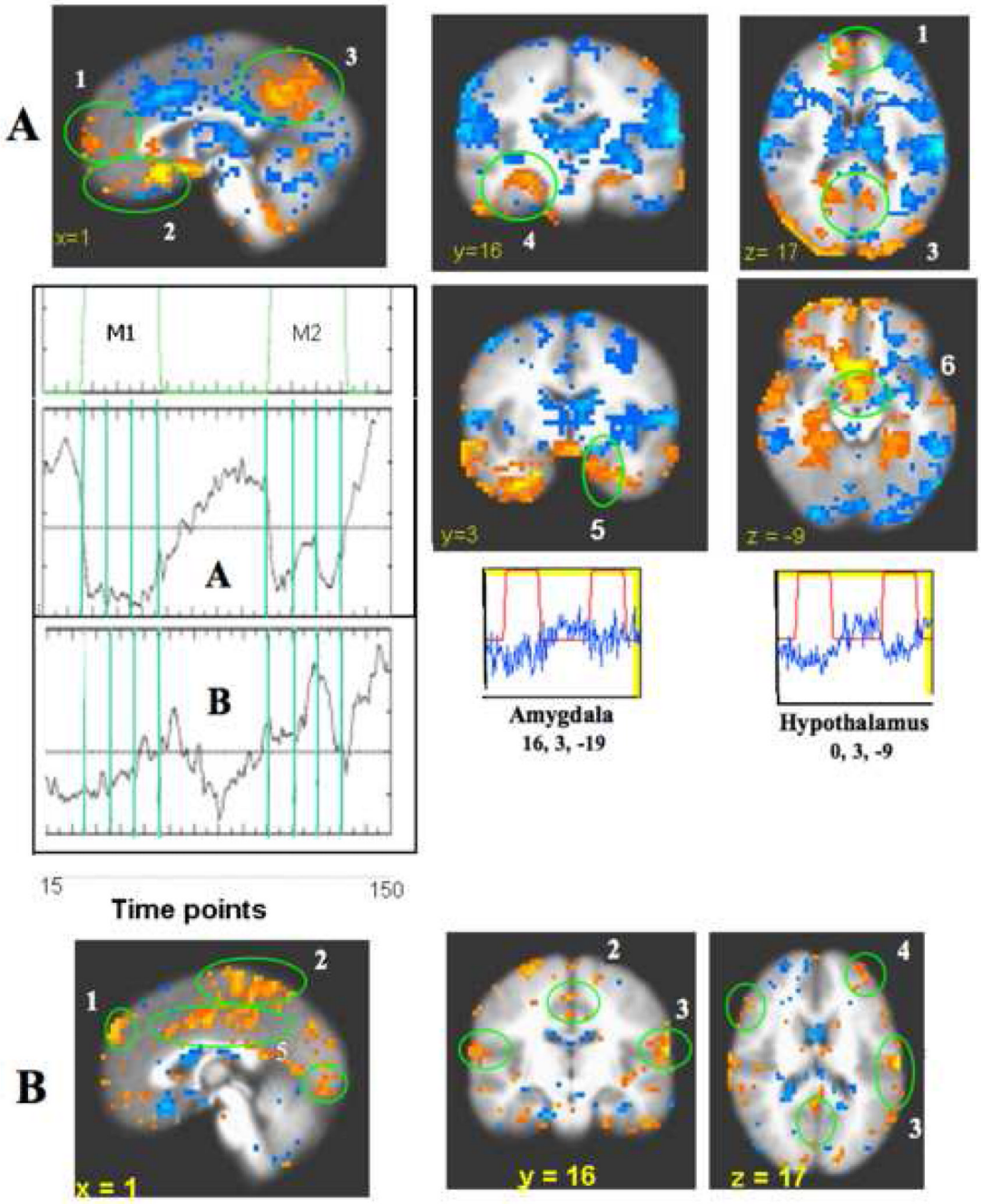

Fig. 5.

Functional connectivity by pICA. Acupuncture at right LI4, ST36 and LV3 in 201 runs on 48 subjects. Time courses derived from pICA are shown for both Deactivation (A) and Activation (B) networks. In addition, the time-course for voxels within the Amy and Hypothalamus from our initial dataset are shown. **A.** Deactivation network. $p < 0.0001$**:** The clusters of deactivated regions in the MPFC (1, 2), MPC (3), and MTL (4, 5) and the Hypo (6) were almost identical in temporal and spatial characteristics to standard GLM and CCA analysis methods. The Amy (5) was involved. **B.** Activation network. $p < 0.005$: Prominent coherent activation occurred in the sensorimotor and association cortices such as the antero-DMPFC (1), SMA/paracentral lobule (2), SII (3), DLPFC (4), and midC/postC_BA23d (5)

are shown. Correlation is seen across hemispheres. ICA was used for generalized trend and pattern across-checking purposes, not primary analyses. The colors follow general trends with reds-yellows representing increasing positive correlation and blues (dark-light) representing increasing anti-correlation.

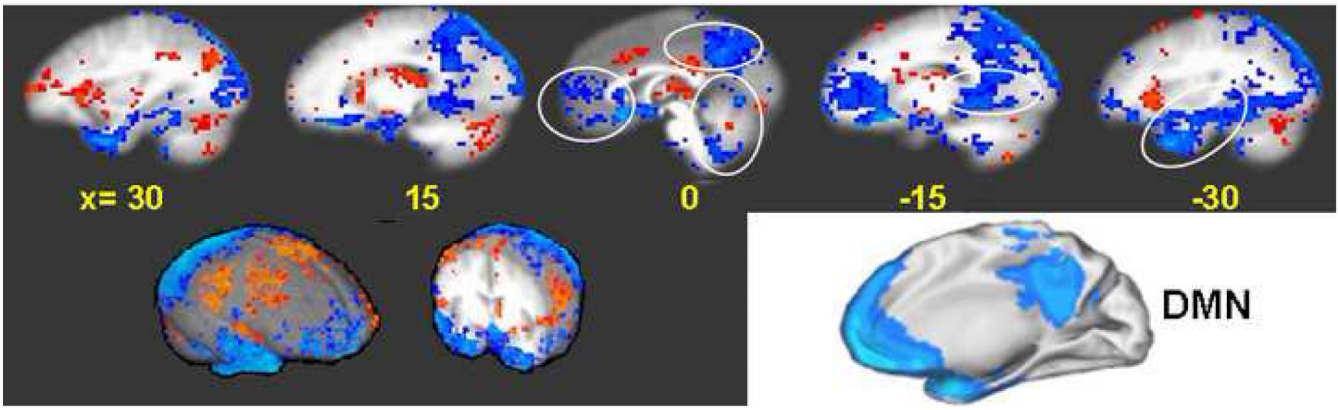

Fig. 6.

Overlap between the LPNN deactivation network in acupuncture by GLM analysis show virtually identical patterns with the DMN. The cortico-limbic response in the MPFC (1), PMPC (2), RSC (3) MTL (4) and cerebellar vermis converge with each other. Synthesis of the regions of correlated deactivation exhibits a view that is remarkably similar to the DMN described for the human brain (Schulman et al 1977). $p < 0.0001$. 3-D views of brain surface and a coronal section through the anterior commissure during acupuncture at right LI4, ST36 and LV3 on 37 subjects exhibit extensive deactivation of the prefrontal, posterior parietal and temporal lobes (encoded in blue) coupled with moderate activation of the sensorimotor cortices and thalamus (encoded in red).

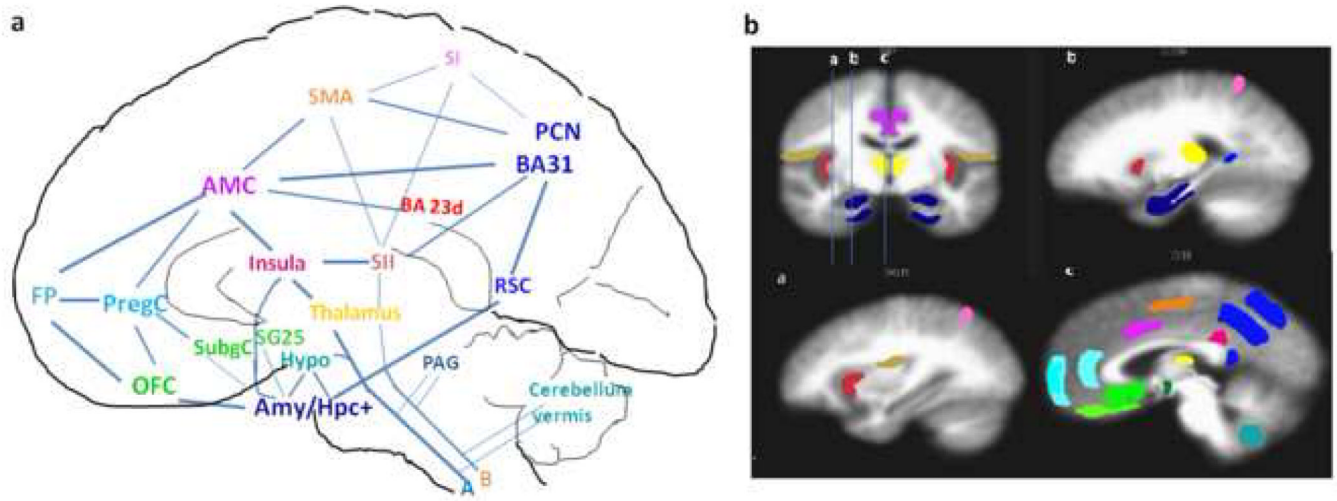

Fig. 7.

Functionally anticorrelated brain networks involved in acupuncture action. In the schematic diagram of a mid-sagittal section (Fig a), deactivated regions are color-coded in cool colors (blue/green) and activated regions in warm colors (red, etc) The areas corresponding to those in the schematic diagram are shown in the MRI sections in Fig b, a coronal slice through the amygdala and 3 sagittal slices as indicated on the coronal section. Regions of deactivation in the limbic-paralimbic-neocortical network (LPNN) aggregate in the medial prefrontal cortex { frontal pole (FP), pregenual and subgenual cingulate (pregC, subgC), subgenual area (SG25), orbitofrontal cortex (OFC)}, medial parietal cortex {precuneus (PCN), post-cingulate_ BA31) }, retrosplenial cortex (RSC)_BA29,30, and medial temporal lobe {amygdala (Amy), hippocampal formation (Hpc+), located lateral to the schematic section}. The hypothalamus, pontine nuclei and cerebellar vermis also showed deactivation. The SII, right anterior insula, antero-middle cingulate (AMC), supplementary motor area (SMA), posterior cingulate_BA23 dorsal, and sensory divisions of the thalamus comprise the activation network. Several associated cortical areas and the basal ganglia showing activation or deactivation are not shown. The figure is partly adapted from Apkarian's figure on pain perception and regulation (Apkarian et al., 2005)

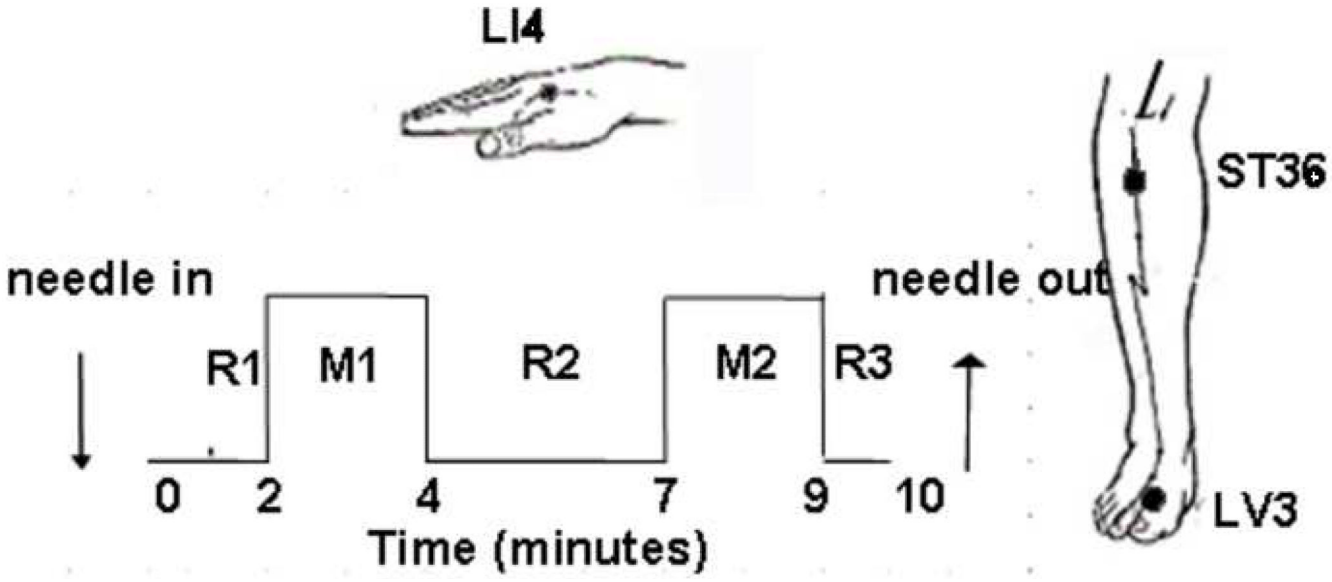

Fig. 8.

Acupoints and time-course paradigm. Manual acupuncture was administered to the LI4, ST36 and LV3 acupoints on the right side, acquiring duplicate scans on each acupoint. The needle remained in place at R1, R2 and R3 (2, 3, 1 minute respectively) and rotated with even motion for 2 min at the rate of 60 times per minute during M1 and M2. The needle was left in place during the sensations interview before starting the second scan. The procedure on each acupoint lasted about 25 min. Tactile stimulation was delivered to the acupoint with a size 5.88 von Frey monofilament using a matched paradigm.

Table I

The BOLD fMRI response to acupuncture and tactile stimulation was matched for acupoints at right LI4, ST36, LV3 in 37 subjects. The spatial distribution and direction of signal change showed overlap in a large subset of structures between the procedures in the deactivation and activation networks. However, results of a paired-t-test demonstrated that the degree of response as measured by the peak % signal change as well as the % of the structural volume involved was significantly greater in acupuncture than in tactile stimulation. In addition to the many structures commonly described as core regions of the DMN, the amygdala and hypothalamus were also involved (A). The same was true for the right anterior insula and divisions of the cingulate cortex in the activation network. The contralateral somatosensory cortex was an exception, as its activation was stronger in tactile stimulation than in acupuncture (B). t* is the value taken from the voxel with maximal signal change in the structure. Numbers in blue = signal decrease, red = increase.

Precuneus	L	BA7m	−2	−62	46	−16.0	−0.2	77.0	−3	−65	31	−11.5	−0.14	57.7	−2.87	0.01
	R		5	−60	50	−17.5	−0.2	90.4	10	−61	49	−10.9	−0.18	50.3	−2.44	0.02
Posterior cingulate	L	BA31	−53	−53	38	−19.3	−0.2	61.0	−2	−47	39	−6.6	−0.10	32.8	−2.08	0.04
	R		2	−53	36	−22.3	−0.2	51.6	3	−63	31	−6.2	−0.11	17.2	−2.49	0.02
Dorsomed prefrontal cortex	L	BA9m	−6	56	26	−6.5	−0.1	11.9	nil						−2.12	0.04
	R		7	53	17	−9.6	−0.1	21.6	7	49	32	−4.6	−0.08	5.7	−2.41	0.02
Frontal pole	L	BA10	−7	58	−2	−10.9	−0.2	37.9	−16	59	0	−4.6	−0.10	3.4	−2.20	0.03
	R		2	55	−7	−10.3	−0.2	49.5	11	62	1	−6.7	−0.10	14.0	−2.85	0.01
Pregenual cingulate	L	BA32/24	−6	35	14	−14.6	−0.2	43.9	−4	34	14	−5.0	−0.09	2.9	−2.62	0.01
	R		5	34	9	−10.2	−0.2	76.3	5	34	−2	−6.0	−0.09	17.5	−2.55	0.01
Subgenual cingulate	L	BA32/24	−5	20	−12	−14.0	−0.3	26.1	−6	25	−10	−7.2	−0.12	4.3	−1.76	−0.10
	R		12	23	−12	−21.1	−0.40	45.5	5	22	−14	−11.6	−0.35	27.3		
Orbitofrontal cortex	L	BA11	−13	33	−18	−11.5	−0.3	6.7	−11	29	−16	−13.8	−0.29	3.7	−2.31	0.02
	R		15	23	−13	−19.3	−0.4	31.9	17	28	−13	−13.4	−0.26	23.4	−2.22	0.03
Subgenual area	L	SG25	−4	17	−10	−22.7	−0.4	53.8	−5	17	−12	−17.8	−0.45	46.2		
	R		5	17	−15	−22.1	−0.61	66.7	6	14	−12	−16.5	−0.55	40.0	−2.32	0.02
Temporal pole	L	BA38	−31	8	−34	−24.4	−0.3	38.6	−34	19	−31	−17.6	−0.28	35.2		
	R		40	13	−31	−23.9	−0.3	57.4	42	13	−25	−10.9	−0.14	36.7	−2.01	0.04
Amygdala	L	BA34	−16	1	−17	−5.2	−0.2	8.3	−19	−3	−22	−6.5	−0.10	6.3		
	R		20	2	−16	−4.8	−0.15	23.2	nil						−2.10	0.04
Hippocampus	L		−22	−8	−19	−11.8	−0.1	35.2	−16	−10	−10	−6.0	−0.11	35.2		
	R		25	−11	−16	−10.6	−0.1	32.5	23	−10	−19	−8.1	−0.12	25.2		
Parahippocampus	L	BA28/36	−29	−23	−16	−8.14	−0.1	28.4	−24	−30	−32	−8.48	−0.11	25.9	−2.01	0.05
	R		27	−28	−18	−7.84	−0.12	33.3	28	−25	−20	−7.8	−0.13	15.1	−2.55	0.01

Angular gyrus	L	BA39	−47	−70	29	−13.4	−0.25	17.6	−48	−69	30	13.0	−0.15	18.6		
	R		47	−66	29	−15.1	−0.26	29.3	46	−67	32	−9.1	−0.15	14.4		
Hypothalamus	L		−4	−1	−9	−9.2	−0.20	27.3	−4	1	−6	−4.1	−0.10	9.1	−2.07	0.04
	R		3	−1	−10	−13.0	−0.3	45.5	nil						−2.75	0.01
Cerebellar vermis	lobule VII		−2	−71	−27	−9.28	−0.2	30	nil							
B. Activation Network																
SII, operculum	L	BA43	−60	−12	18	6.3	.11	34.5	−56	−12	13	10.8	0.20	70.2	1.97	0.05
	R		nil						nil						nil	
SII, inferior parietal	L	BA40	−59	−20	17	11.62	0.16	28.2	−59	−21	16	16.2	0.23	50.7	2.61	0.01
	R		61	−19	19	7.85	0.16	11.1	62	−30	27	7.6	0.13	29.6	nil	
Anterior insula	L		−28	23	−2	5.15	0.09	5.1	nil						2.03	0.05
	R		29	19	1	14.66	0.16	16.7	nil						2.42	0.02
Middle cingulate	L	BA32	−9	31	32	4.30	0.08	0.7	nil						2.25	0.03
	R		nil						nil						2.11	0.04
Posterior cingulate	L	BA23d	−4	−31	23	6.33	0.12	15.0	nil						2.53	0.01
	R		3	−29	27	6.76	0.13	19.4	nil						nil	
Thalamus	L		−7	−7	5	5.29	0.09	9.1	nil						2.04	0.04
	R		5	−7	5	5.00	0.10	3.9	nil			3.6	0.10	.6	2.04	0.04

Table 2

The BOLD fMRI response in *deqi* (52 runs in 37 subjects) was compared with *deqi* plus sharp pain (52 runs in 29 subjects) during acupuncture at right LI4, ST36, LV3, using a voxel by voxel two sample t-test. In the deactivation network , the presence of pain attenuated the signal decrease of most structures (thresholded at $p < 0.05$). The hypothalamus, left amygdala, cerebellar vermis became activated instead (Fig A). In the activation network, the somatosensory cortex signal increase was enhanced while activation of the right anterior insula and divisions of the cingulate cortex was attenuated on by pain (Fig B). t* is the value taken from the voxel with maximal signal change. Numbers in blue = signal decrease, red = increase.

			Deqi					Mixed					t-test	
							%Sig Δ					%Sig Δ	%Sig Δ	
Brain Structure	**Side/Area**		**x**	**y**	**z**	**t***	**%**	**x**	**y**	**z**	**t***	**%**	**t**	**p <**
A. Deactivation Network														
Posterior cingulate/	L	BA31/7m	−2	−53	38	−20.2	−0.14	−2	−53	33	−4.8	−0.1	3.19	0.002
Precunious	R		3	−55	35	−20.8	−0.14	3	−53	33	−6.1	−0.13	3.32	0.001
Pregenual cingulate/	L	BA32/10	−3	43	2	−9.5	−0.08	−2	46	2	−7.3	−0.12	3.2	0.002
Frontal pole	R		5	37	8	−11.3	−0.08	3	46	2	−8	−0.12	3.29	0.001
Subgenual area	L	SG25	−3	20	−12	−25.6	−0.52	−2	11	−9	−19	−0.63	2.19	0.032
	R		4	18	−12	−35.5	−0.51	4	14	−10	−15.6	−0.42	2.14	0.034
Orbitofrontal cortex	L	BA11	−3	40	−18	−13	−0.16	nil					2.05	0.044
	R		5	52	−21	−20.4	−0.54	nil					2.31	0.004
Temporal pole	L	BA38	−28	19	−32	−26	−0.34	−32	18	−32	−7.6	−0.15	3.31	0.001
	R		35	19	−33	−25.8	−0.32	64	20	−30	−18.7	−0.3	3.19	0.002
Amygdala	L	BA34	−21	−6	−20	−14.3	−0.9	−25	5	−12	4.8	0.12	3.91	0.001
	R		22	−8	−12	−13.6	−0.08	17	5	−15	−7	−0.12	2.63	(0.010)
Hippocampus	L		−18	−11	−15	−12.7	−0.08	nil					3.63	0.001
	R		18	−11	−14	−12.7	−0.11	20	−16	−12	−5	−0.1	3.35	0.001
Parahippocampus	L	BA28/36	−23	−11	−22	−7.9	−0.07	nil					2.96	0.004
	R		19	−7	−25	−11.6	−0.12	25	−22	−21	5.9	0.24	2.52	0.014
Hypothalamus	L		−1	−2	−8	−20.2	−0.2	−1	−4	−7	5.9	0.12	3.88	0.001
	R		2	−2	−8	−18.6	−0.2	2	−6	−6	5.8	0.14	3.27	0.002
Cerebellar vermis	lobule VII		−1	−79	−30	−7.9	−0.16	−1	−71	−21	11	0.15	3.52	0.001
	lobule VIII		−1	−65	−37	−6.5	−0.12	−1	−63	−27	9.3	0.14	3.66	0.001
B. Activation Network														

			Deqi					Mixed					t-test	
						%Sig Δ					%Sig Δ		%Sig Δ	
Brain Structure	**Side/Area**		**x**	**y**	**z**	**t***	**%**	**x**	**y**	**z**	**t***	**%**	**t**	**p <**
SII, operculum	L	BA43	−61	−12	20	15.4	0.16	−62	−13	17	17.09	0.33	3.73	0.001
	R		59	−12	20	6.7	0.05	55	−6	11	7.4	0.14	ns	
SII, inferior parietal	L	BA40	−59	−21	22	19.8	0.16	−64	−25	20	15.7	0.42	5.4	0.001
	R		54	−21	25	13.3	0.1	55	−25	26	13	0.16	3.51	0.001
Ant middle cingulate/DMPFC	L	BA32/10	nil					−2	22	41	11	0.15	3.91	0.001
	R		4	27	37	7.8	0.07	1	31	34	10	0.15	5.93	0.001
Ant middle cingulate	L	BA24	−3	14	32	7.4	0.08	−3	19	27	6.9	0.1	2.91	0.005
	R		3	11	34	6.2	0.07	2	18	31	7.6	0.15	3.95	0.001